

Article

Carbon Dioxide Separation by Polyethylene Glycol and Glutamic Acid/Polyvinyl Alcohol Composite Membrane

Angus Shiue ^{1,†}, Ming-Jie Yin ^{2,†}, Min-Hsuan Tsai ¹, Shu-Mei Chang ^{1,3,*} and Graham Leggett ⁴

- ¹ Graduate Institute of Organic and Polymeric Materials, National Taipei University of Technology, Taipei 106, Taiwan; angusshiue@gmail.com (A.S.); minhsuantsai@ntu.edu.tw (M.-H.T.)
- ² Beijing Key Laboratory for Green Catalysis and Separation, Department of Environmental and Chemical Engineering, Beijing University of Technology, Beijing 100124, China; yinmj@bjut.edu.cn
- ³ Department of Molecular Science and Engineering, Research and Development Center for Smart Textile Technology, National Taipei University of Technology, Taipei 106, Taiwan
- ⁴ LI-COR Biosciences, Cambridge CB4 0WS, UK; graham.leggett@licor.com
- * Correspondence: f10914@mail.ntut.edu.tw; Tel.: +886-2-2771-2171 (ext. 2408)
- † Denotes equal contribution.

Abstract: In this study, Polyvinyl alcohol (PVA) blended with Polyethylene glycol (PEG), Monosodium glutamate (MSG) and Glutamic acid (GA) was cast on a reverse osmosis membrane to form a composite membrane. It is expected that the ether group can increase the CO₂ affinity of the membrane. Sodium tetraborate (Borax) as a crosslinker can increase membrane basicity and glutamic acid (salt) can provide an enhanced transport mechanism, thereby improving the permeability and selectivity of carbon dioxide. FTIR spectra show that the thickness of coating is sufficiently low, while SEM results show that PVA-PEG series have a dense surface, and particles are observed on the surface of MSG/GA series. The gas permeance and separation performance of the composite membrane was tested using a single gas. Results showed that CO₂ had higher permeance (GPU) at lower pressure differential. PEG with an ether group had the greatest effect on improving CO₂ permeance and selectivity. However, MSG and GA with amine groups could not effectively improve CO₂ selectivity due to solubility. The best coating solution was provided by PVA-PEG-1.2. The CO₂ selectivity of the composite membrane was 10.05 with a pressure differential of 1.00 bar in a humid environment and no obvious deterioration was observed over a 10-day period. Borax can improve selectivity, water absorption, and thermal stability while avoiding the need for high temperature and long crosslinking time of aldehydes, which makes it possible to be used in a PVA carbon dioxide separation membrane.

Keywords: carbon dioxide; polyvinyl alcohol; polyethylene glycol; Borax; monosodium glutamate; glutamic acid; reverse osmosis membrane



Citation: Shiue, A.; Yin, M.-J.; Tsai, M.-H.; Chang, S.-M.; Leggett, G. Carbon Dioxide Separation by Polyethylene Glycol and Glutamic Acid/Polyvinyl Alcohol Composite Membrane. *Sustainability* **2021**, *13*, 13367. <https://doi.org/10.3390/su132313367>

Academic Editors:
Avelino Núñez-Delgado,
Zhien Zhang, Elza Bontempi,
Mario Coccia, Marco Race and
Yaoyu Zhou

Received: 6 October 2021
Accepted: 30 November 2021
Published: 2 December 2021

Publisher's Note: MDPI stays neutral with regard to jurisdictional claims in published maps and institutional affiliations.



Copyright: © 2021 by the authors. Licensee MDPI, Basel, Switzerland. This article is an open access article distributed under the terms and conditions of the Creative Commons Attribution (CC BY) license (<https://creativecommons.org/licenses/by/4.0/>).

1. Introduction

The increasing demand for energy and an associated need to improve efficiency of energy consuming processes has led to a growing global willingness to use membrane materials as a potential long-term solution to reduce greenhouse gas emissions and prevent global warming. With global energy consumption expected to double by 2050, current fossil fuel reserves are under increasing environmental and economic pressure. The energy sector must unequivocally overcome the many technological barriers between membrane production, utilization, and potential applications. Polymer substrate membranes are one of the most popular separation materials in the industry, but their low temperature and chemical stability greatly limit their application. Despite these limitations, demand for inorganic gas permeable membranes is increasing in many cases. Carbon membranes are particularly useful in gas separation through adsorption and molecular screening mechanisms, even between gases of very similar molecular size [1–4]. However, in industrial applications, they suffer from low penetration and poor mechanical strength. To date,

the utilization of polymer membranes in pilot plants and at industrial scales has been limited due to higher manufacturing costs. Therefore, to compensate for the high cost, manufacturers have explored ways to improve the separation performance of membrane materials for various gases [5,6].

Each membrane material has its advantages and challenges in terms of material cost, separation performance, and service life. The development of advanced membrane materials to increase cost-effectiveness is critical to reducing CO₂ capture costs. Each membrane material has its own separation characteristics, thermochemical stability, and mechanical strength [7]. In general, most polymer membranes have good separation properties and relatively low costs, but the low stability of the membrane is a negative performance factor when exposed to acidic gases and harsh conditions (high temperature and high pressure), typical in many industrial processes.

Existing gas separation membranes must further improve permeability and selectivity to expand their market share and compete with traditional separation technologies. Since gas permeability is inversely proportional to the thickness of the dense layer, a high multi-layered material must be selected, or the thickness of the dense selective layer reduced to prepare a more efficient membrane. However, highly permeable materials typically exhibit low selectivity due to the trade-off between the permeability and selectivity of polymer materials [8,9]. Porous membranes may consist of a thin film composite (TFC) consisting of one or more layers of a porous substrate to maximize selectivity, permeability, and mechanical crosslinking, or a more traditional asymmetric film construction where a fine porous skin layer is applied to a thick microporous underlying layer. TFC construction offers a low skin advantage: (1) only a small amount of selective layer material, less than 2 g/m², is required to coat the surface of a porous substrate, compared to approximately 50 g/m² required to manufacture the overall skinning of an asymmetric film—therefore, the cost of materials is reduced when applying TFC construction; (2) depending on the product requirements, each layer of the membrane layer can be tuned for optimal separation; (3) as long as the main body of the membrane can form or deposit on the surface of the substrate thin layer, its mechanical properties and machinability restrictions are less. However, the manufacture of high-performance, defect-free TFC materials is challenging: (1) there are some challenges in the influence of substrate resistance; (2) performance is compromised if the thickness of the ultra-thin selective layer is inconsistent; (3) material intrusion sub-strategy; (4) ultra-thin selective layers accelerate aging and plasticization, and these harmful problems may degrade the performance of TFC [10–13].

Compared with the membrane after the solution diffusion mechanism, the promotion of the transmission mechanism contributes to high CO₂ separation and CO₂/N₂ selectivity. In convenient transport, the CO₂ separation capacity of a mobile carrier is higher than that of a fixed carrier, but lacks carrier stability [14]. Polyallylamine (PAA) is one of the fixed carriers used for CO₂ separation and is mixed with other polymers, either without change or in the form of bit resistance [15–21]. PAA is primarily amine-based, which is very fragile and cannot form a membrane under dry conditions. The polyvinyl alcohol (PVA), in combination with PAA, is widely used as a fixed position in CO₂ substrates and mixing bases [18]. Temperature and humidity influence the transport mechanism. PVA is soluble in water and at higher humidity a decrease in CO₂ emission performance may be observed at temperatures lower than 70 °C [15].

Polyethylene oxide (PEO) membranes are considered attractive materials for CO₂ separation because the polymer chain has polar ether-oxygen bonds and therefore it has a strong CO₂ affinity [22]. Great efforts have been made in the design and synthesis of polymers containing PEO. Hirayama et al. [23] synthesized films containing PEO and crosslinking polymers with a CO₂/N₂ selectivity of 69 and a CO₂ penetration rate of 62 Barrer. Potreck et al. [24] argue that PEO-based block congregations provide an attractive way to integrate CO₂ separation using thin-film technology because of the high interaction between CO₂ and its polar ether connections.

In this study, polyvinyl alcohol was chosen to make the main polymer. It is a convenient polymer to use, being non-toxic and water soluble. Polyglycol was selected to increase the solubility coefficient and CO₂ affinity. To avoid high molecular weight leading to crystallization and reduction in the permeability of CO₂, liquid PEG200 was used in the preparation of the membrane. In addition, consideration was given to the pH value of the membrane and reduction of cross-link reaction time and temperature. To this end, polyvinyl alcohol was chosen, as cross-linking occurs at room temperature. In addition, tetraborate (Borax) was employed as a crosslinking agent. Once prepared, the composite membrane was tested to determine carbon dioxide permeability and selectivity in both dry and humid environments. Monosodium glutamate (MSG), which is expected to promote transport mechanisms and therefore increase CO₂ permeability and selectivity of the composite membrane was also tested, while glutamic acid (GA) was also used in experiments to compare the effects of glutamic acid (salt).

2. Materials and Methods

2.1. Chemicals and Equipment

Polyvinyl alcohol (PVA) ($M_w = 31,000\text{--}55,000$ g/mol, 98.0~98.8% hydrolyzed), polyethylene glycol (PEG) ($M_w = 200$ g/mol), sodium tetraborate (Borax), monosodium glutamate (MSG), and glutamic acid (GA) were purchased from Acros Organics, Geel, Belgium. All chemicals were used as received without treatment and deionized water was used as the solvent during preparation. The reverse osmosis membrane was purchased from Film Tec Corp. Minneapolis, MN, USA. N₂ and CO₂ applied in the experiments were purchased from Chin-Fung Ltd., Taipei, Taiwan.

2.2. Structure of Composite Membrane

Reverse osmosis membrane was used as a substrate and coated with a polymer-mixed solution to make a composite membrane. The uppermost layer of this composite membrane was dominated by polyvinyl alcohol (PVA), mixed with polyethylene glycol (PEG). Monosodium glutamate (MSG) or glutamic acid (GA) was an optional layer to contact the air, interacting with CO₂ via its quadrupole moment. Gas penetration and separation were achieved via a dissolve diffusion mechanism. The reverse osmosis membrane was a polyamide layer about 200 nanometers thick and had approximately a 15 nanometers aperture from top to bottom, followed by a porous polysulfone (PSU) layer approximately 40 microns thick, with polyester at the bottom as a support layer approximately 120 microns thick.

2.3. Preparation of Polymer-Mixed Solution

In this experiment, a fixed PVA intake was configured in different proportions by adjusting the amount of PEG, MSG, GA, Borax, and deionized water. The polymer-mixed solution was divided into four preparation methods: (a) only used PVA and Borax (b) added PEGs and adjusted the combination of proportions (c) added MSGs and adjusted the combination of proportions and (d) added GA and adjusted the combination of proportions.

2.4. Preparation of Self-Supporting Membrane

A polymer-mixed solution was prepared with a micro straw of 10 mL, transferred to a petri dish and left in a drying chamber for 48 h, then placed in a vacuum oven (-700 mmHg) to dry for 24 h at 35 °C. The membrane was removed and baked in a hot air oven for 1 h at a temperature of 105 °C to remove the remaining moisture. This completed the preparation of the self-supporting membrane.

2.5. Preparation of Composite Membrane

A substrate reverse osmosis membrane (about 15 × 20 cm) was fixed to the glass plate, and then the prepared polymer-mixed solution was applied to this membrane with a plastic form coated rod. The modified substrate was placed in a drying oven for 24 h

before being transferred to a vacuum oven (-00 mmHg) at 35 °C where it was further dried for 24 h. This process resulted in a polymer membrane formed on the substrate surface. After making a polymer membrane, Fourier-Transform Infrared Spectroscopy-Attenuated Total Reflection (FTIR-ATR, using SHIMADZU IRSpirit with QATR-S module), Thermogravimetric Analysis (TGA, using NETZSCH TG 209 F3), and Scanning Electron Microscopy (SEM, using HITACHI TM4000Plus) were used to confirm surface modification on the reverse osmosis membrane.

2.6. CO₂ Permeation Test

The gas membrane permeation system device is shown in Figure 1. Pure N₂ or pure CO₂ gas enters the line via a float flow control valve. The inlet pressure into the system is controlled by means of a precision pressure control valve, with pressure measured by a pressure meter. The pipeline is divided into two paths. One path is through a deionized water humidifier. The humidifier consists of a water vessel immersed in a thermostatic tank set at 35 °C. Gas is passed through the water to achieve a relative humidity (RH) of approximately 80%. After the humidifier, the gas and moisture enter the gas penetration device which contains the membrane to be tested. The gas penetration device is placed in the hot air oven and this is set to a fixed temperature. This temperature is maintained for the duration of the experiment to reduce any changes in membrane performance that may arise from temperature fluctuations. The lower end of the gas penetration device is connected with a three-way valve and the mass flow meter (Brooks Instrument, Hatfield, PA, USA) of the two gases is attached at each end, allowing evaluation of the performance of the membrane under test. During operation, the test gas can be humidified or dry, depending on the selected flow path as shown in Figure 2.

When a gas passes through a dense membrane, transport is mostly explained by the solution-diffusion model. A formula describing the passing properties of the gas, called permeability of the gas, is derived from Fick's first law of diffusion theorem.

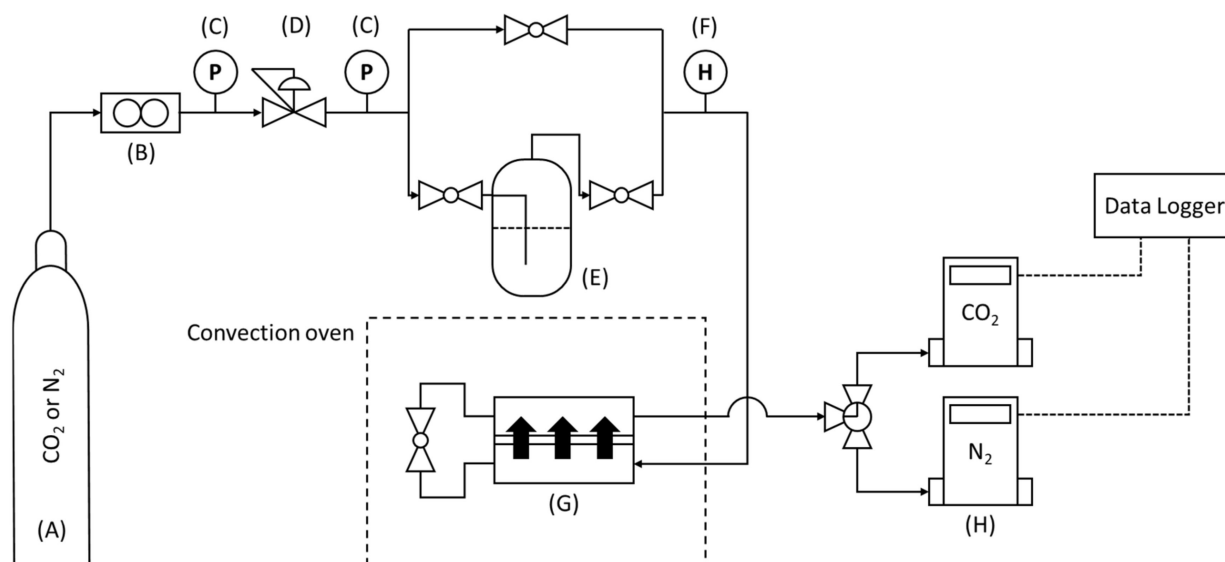


Figure 1. Schematic diagram of the polymer membrane separation system. (A) N₂ or CO₂, (B) floating flow controller, (C) pressure gauge, (D) precision regulator, (E) humidifier, (F) temperature and humidity meter, (G) membrane separation system, and (H) mass flow meter.

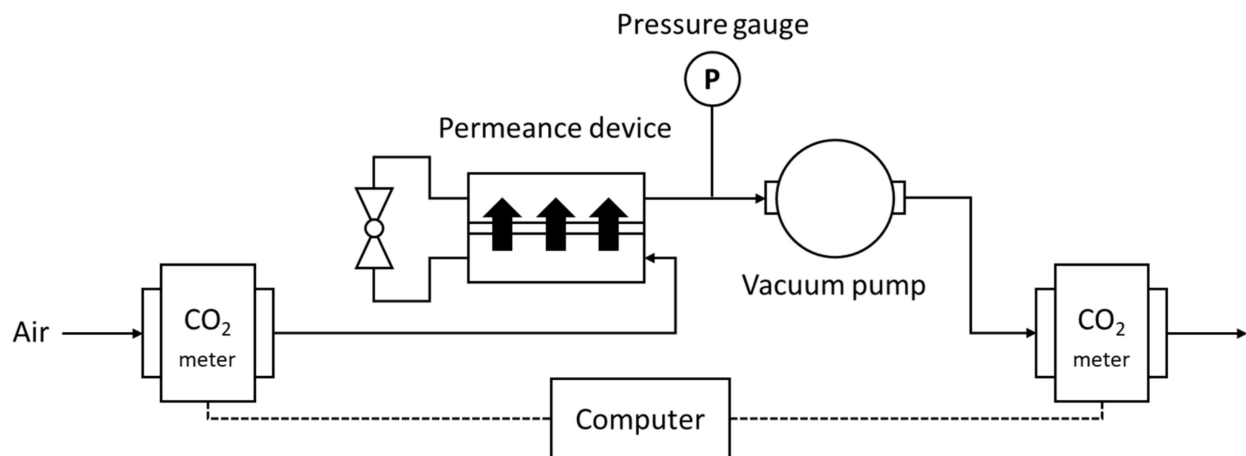


Figure 2. CO₂ membrane separation energy measurement system.

2.7. Principle

When a gas passes through a dense membrane, its behavior is mostly explained by the solution-diffusion model, and the membrane material itself has a formula for the passing properties of the gas, called the permeability of the gas, which is derived from Fick's first law of diffusion theorem:

$$J = -D \frac{\partial c}{\partial x} \quad (1)$$

where J is the gas flux ($\text{cm}^{-2} \text{s}^{-1}$), D is the gas diffusion coefficient in the membrane ($\text{cm}^2 \text{s}^{-1}$), and $\frac{\partial c}{\partial x}$ is the concentration gradient (cm^{-4}).

The boundary condition is

$$x = 0, C = C_1 \quad (2)$$

$$x = L, C = C_2 \quad (3)$$

where x is length scale of the system (m), and L is the thickness of the membrane (cm). The concentration distribution of gas molecules in the membrane (mol m^{-3}) can be solved by boundary conditions as shown in the following equation:

$$\frac{C - C_1}{C_2 - C_1} = \frac{x}{L} \quad (4)$$

Equation (4) is substituted into Equation (3) to obtain the gas flux (J).

$$J = -D \frac{(C_1 - C_2)}{L} \quad (5)$$

The physical significance of the gas flux is the area per unit, the number of gas molecules passed in a unit time:

$$J = \frac{1}{A} \frac{\partial n}{\partial t} \quad (6)$$

Combine Equations (5) and (6) to obtain:

$$\frac{1}{A} \frac{\partial n}{\partial t} = -D \frac{(C_2 - C_1)}{L} \quad (7)$$

Assuming that the dissolution and evaporation of the gas is balanced, the concentration at the membrane interface is related to the dispensing of the components in the gas and it must comply with Henry's Law:

$$C' = Sp \quad (8)$$

where C' is the solubility of a gas at a fixed temperature (mL gas L^{-1}), S is the solubility coefficient of the gas for the membrane (mL gas L^{-1}), and p is the partial pressure of the gas (atm).

At constant temperature, $S_1 = S_2 = S$, Equation (8) substituted into (7) obtains:

$$\frac{1}{A} \frac{\partial n}{\partial t} = -D \frac{(S_2 p_2 - S_1 p_1)}{L} = DS \frac{(p_1 - p_2)}{L} \quad (9)$$

The defined permeability coefficient is:

$$P = DS \quad (10)$$

Equation (10) substituted into (9) obtains:

$$\frac{1}{A} \frac{\partial n}{\partial t} = P \frac{(p_1 - p_2)}{L} \quad (11)$$

The gas permeability coefficient P is arranged as:

$$P = \frac{L}{(p_1 - p_2)A} \frac{\partial n}{\partial t} \quad (12)$$

Measurements are usually made in Barrer units:

$$1\text{Barrer} = 10^{-10} \frac{\text{cm}^3(\text{STP}) \cdot \text{cm}}{\text{cm}^2 \cdot \text{sec} \cdot \text{cmHg}} \quad (13)$$

In addition to permeability, the overall permeability of the membrane is often expressed as a gas permeability (Permeance), which is the gas penetration coefficient divided by the membrane thickness L as follows:

$$\text{Permeance} = \frac{\text{Permeability}}{L} = \frac{1}{(p_1 - p_2)A} \frac{\partial n}{\partial t} \quad (14)$$

Its physical significance is described as:

$$\text{Permeance} = \frac{\text{Gas amount}}{\text{Pressure difference} \times \text{Surface Area}} \quad (15)$$

From Equation (15), permeance units can be expressed as $\frac{\text{cm}^3(\text{STP}) \cdot \text{cm}}{\text{cm}^2 \cdot \text{sec} \cdot \text{cmHg}}$. Because this number is small, it is usually expressed in gas Permeance Units (GPUs).

$$1\text{GPU} = 10^{-6} \frac{\text{cm}^3(\text{STP}) \cdot \text{cm}}{\text{cm}^2 \cdot \text{sec} \cdot \text{cmHg}} \quad (16)$$

In addition, the film can be obtained by dividing the gas permeability or gas permeability coefficient of the two gases to obtain membrane selectivity:

$$\text{Selectivity} = \frac{\text{Permeance}(\text{Gas1})}{\text{Permeance}(\text{Gas 2})} = \frac{\text{Permeability}(\text{Gas1})}{\text{Permeability}(\text{Gas 2})} \quad (17)$$

3. Results and Discussion

3.1. FTIR Analysis

3.1.1. Infrared Spectrum of Polyvinyl Alcohol Cross-Linked Borax

Polyvinyl alcohol membrane stretch vibrations of O-H and C-O are found at 3100–3600 and 1730 cm^{-1} , respectively. At 2850–2950 cm^{-1} two C-H symmetrical and asymmetric stretch vibrations are observed, which may result from the undehydrated ethylene acetate group on polyvinyl alcohol. It can be seen that there is a C-H bending vibration at 1350 cm^{-1} , and C-O

stretch vibration feature peaks at 1140 and 1090 cm^{-1} . Cross-linked membranes that have added Borax display similar absorption features, and are shown in Figure 3 and Table 1.

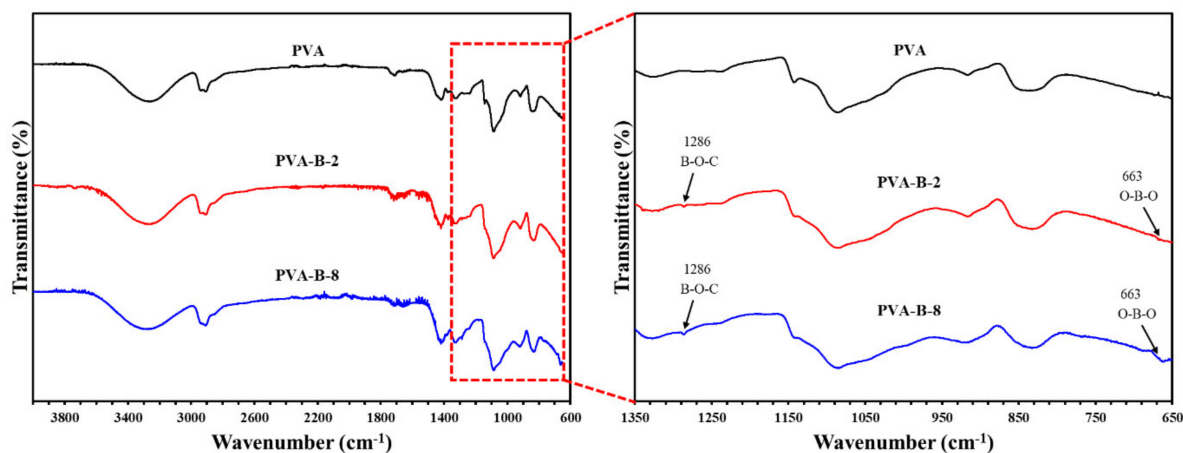


Figure 3. Infrared spectrum of PVA, PVA-B-2, and PVA-B-8 samples.

Table 1. Peak assignments of PVA and cross-linked PVA.

Peak Position (cm^{-1})		Peak Assignment
PVA	PVA-B-Series	
3100–3600	3100–3600	O-H stretching
2850–2950	2850–2950	C-H symmetric/asymmetric stretching
1730	1730	C=O stretching
1350	1350	C-H bending
1140	1140	C-O stretching
1090	1090	C-O stretching
	1286	B-O-C stretching
	663	O-B-O stretching

Since Borax in PVA-B-2 is only 2 percent of its weight relative to polyvinyl alcohol, to further determine the effects of Borax, a self-supporting membrane of PVA-B-8 sample with Borax content of 8 percent is formulated and adjusted. The instrument scanning parameters were measured at a resolution of 0.9 cm^{-1} and absorption peaks could be seen at 1286 cm^{-1} and 663 cm^{-1} , while the PVA-B-2 membrane had a slight decrease in penetration in both locations. The two absorption peaks correspond to B-O-C and O-B-O stretching vibrations, representing boric acid from borax dissolved in water, acting as a cross-linker between polyvinyl alcohols in the process of forming a membrane. This was also observed and reported in previous studies [25–27] as shown in Figure 3 and Table 1.

3.1.2. Experimental Coating and Infrared Spectrum

Because the gas permeability is related to the thickness of the separation membrane under the condition that the gas permeability is constant, the thicker the separation membrane, the lower the gas permeability, and vice versa. FTIR, using a half-attenuation full-reflection device, was used as a means to make a preliminary confirmation that the membrane selection layer was thin enough. A polyvinyl alcohol self-supporting membrane, a reverse osmosis membrane and the experimental method of polyvinyl alcohol as a selection layer, coated as a support layer on the reverse osmosis membrane prepared composite membrane were analyzed.

The reverse osmosis membrane is itself a composite membrane of polyamide and polysulfone. From the spectrum in Figure 4 and Table 2, the reverse osmosis membrane prior to modification is seen to have stretching vibrations of O-H, C-H with alkane, N-H,

C=C, and C-O at 3500–3200, 2966 and 1236, 1560, 1500, and 1050 cm^{-1} , respectively. Characterized absorption that may come from a polycyclic group is: stretching vibration of C=C, C-O-C, O-S-O, C-H, and C-S-C at 1585 cm^{-1} and 1487, 1236, 1149, 1014, and 831 cm^{-1} , respectively [26,28].

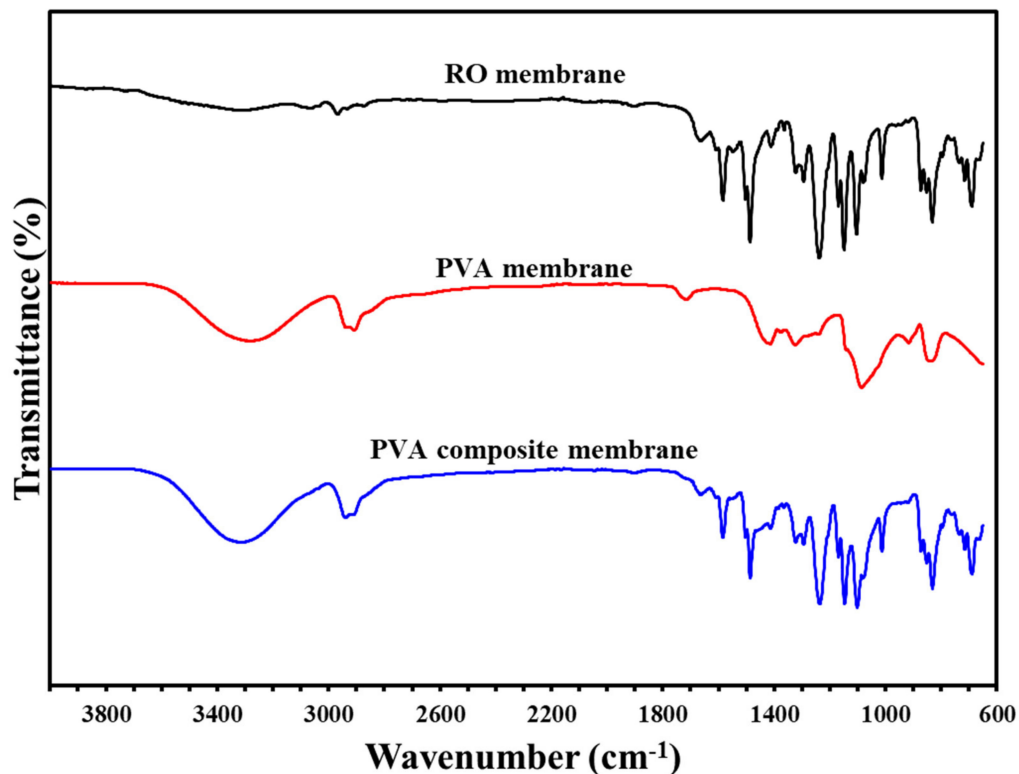


Figure 4. The infrared spectrum of the components of the composite membranes and each layer.

Table 2. Peak assignments of composite membrane.

Peak Position (cm^{-1})	Peak Assignment
3600–3000	O-H stretching
2966	C-H stretching
2950–2850	C-H symmetric asymmetric stretching
1585	C=C stretching
1560	N-H stretching
1500	C=C stretching
1487	C=C stretching
1236	C-O-C stretching
1149	O-S-O stretching
1050	C-O stretching
1014	C-H stretching
831	C-H stretching
690	C-S-C stretching

It is found that the absorption peaks of the reverse osmosis membrane prior to modification is concentrated below 1800 cm^{-1} , although there are absorption peaks above 2700 cm^{-1} , but not strong, while polyvinyl alcohol at 3600–3000 cm^{-1} displays a strong absorption peak of O-H stretching vibration, and there is an absorption peak resulting from the C-H stretching vibration near 2950 cm^{-1} . Therefore, if coated with polyvinyl alcohol, the prepared composite membrane should display absorption features at 3000 cm^{-1} associated with O-H and at 2950 cm^{-1} resulting from C-H groups. The visible composite film results in features in the infrared spectrum, while at the same time peaks associated

with the polyvinyl alcohol selection layer and reverse osmosis membrane support layer are also present. Since infrared spectral measurements are carried out by half-attenuation full reflection, the depth range of infrared light entering the sample is approximately 0.5 to 3 μm (related to the crystal refractive index, sample refractive index, incident angle and number of incident light waves used in the device). From this it can be inferred that the thickness of the coated polyvinyl alcohol selection layer should be less than 3 μm , as shown in Figure 4 and Table 2.

3.1.3. Infrared Spectrum of Polyvinyl Alcohol-Polyethylene Glycol

A fixed amount of polyvinyl alcohol was mixed with different volumes of polyethylene glycol and applied to a self-supporting membrane. The resulting materials were analyzed using ATR-FTIR; results are shown in Figure 5. The main absorption peaks of polyethylene glycol are C-H and C-O stretching vibrations at 2800–2900, and 1350 and 1090 cm^{-1} , respectively. From the spectrum, it is observed that increasing the polyglycol addition results in strengthening of the absorption features associated with polyethylene glycol. This is especially evident for C-H and C-O stretching vibrations at 2800–2900 and 1090 cm^{-1} , respectively.

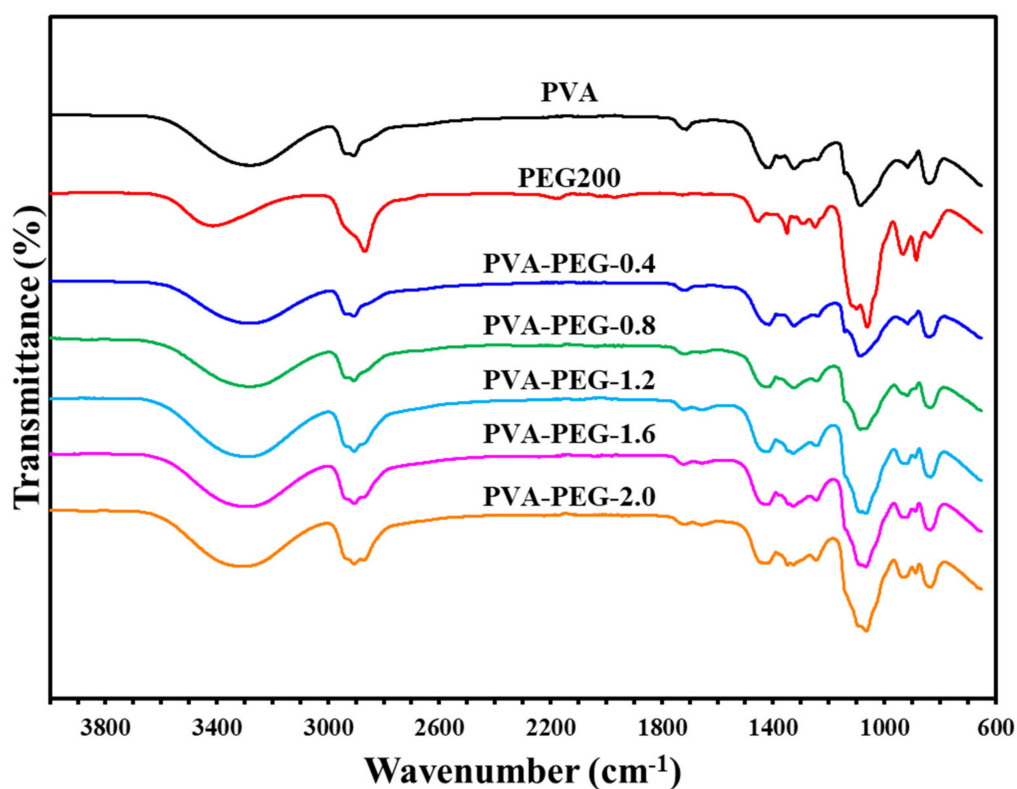


Figure 5. Infrared spectrum of polyvinyl alcohol-polyethylene glycol self-supporting membranes.

A mixed solution of polyvinyl alcohol and polyethylene glycol was coated on the reverse osmosis membrane to prepare a composite membrane. ATR-FTIR was used to analyze the resulting materials; results are shown in Figure 6. The characteristic absorption features of the reverse osmosis membrane are observed, confirming that the coating is thin enough to allow infrared light to penetrate the selection layer to the reverse osmosis membrane. The strength of the absorption line at 1090 cm^{-1} is dependent on the amount of polyglycol in the sample.

3.1.4. Infrared Spectrum of Polyvinyl Alcohol–Sodium Glutamate

A fixed amount of polyvinyl alcohol was mixed with different weights of monosodium glutamate and prepared into a self-supporting membrane, which was analyzed by ATR-FTIR; results are shown in Figure 7. The presence of MSG is evident from the peaks at 1602 and 1395 cm^{-1} from the absorption of C-O stretching vibrations. It can be found that as the amount of added MSG increases, so the strength of the characteristic absorption feature associated with monosodium glutamate increases, resulting from the self-supporting membrane of PVA-MSG.

Polyvinyl alcohol is mixed with monosodium glutamate and coated in a reverse osmosis membrane to form a composite membrane; its infrared spectra are shown as Figure 8. Compared with the original reverse osmosis membrane, the composite membrane spectrum displays polyvinyl alcohol absorption lines, and the sodium glutamate C-O stretching vibration of 1602 cm^{-1} . Penetration also decreased with an increase in the content of sodium glutamate, and from another C-O stretching vibration at 1395 cm^{-1} , it can be seen that the absorption peak becomes more obvious, representing an increase in the MSG content in the selection layer.

3.1.5. Infrared Spectrum of Polyvinyl Alcohol–Glutamic Acid

Since a layer of crystallization is observed on the surface of the membrane when it is prepared for self-supporting membranes, only composite membrane spectra are shown in Figure 9 and Table 3. The glutamic acid itself is visible from absorption lines at 2950–3050 cm^{-1} from C-H, N-H or COOH, symmetrical N-H, and symmetrical COOH stretching vibration at 1635, 1500, and 1400 cm^{-1} , respectively [29]. However, the absorptions resulting from these groups are not strong. The glutamate acid addition is low and thus an increase in strength of absorption features associated with this compound are not observed as the added amount is increased. There is also no change in penetration related to the added amount.

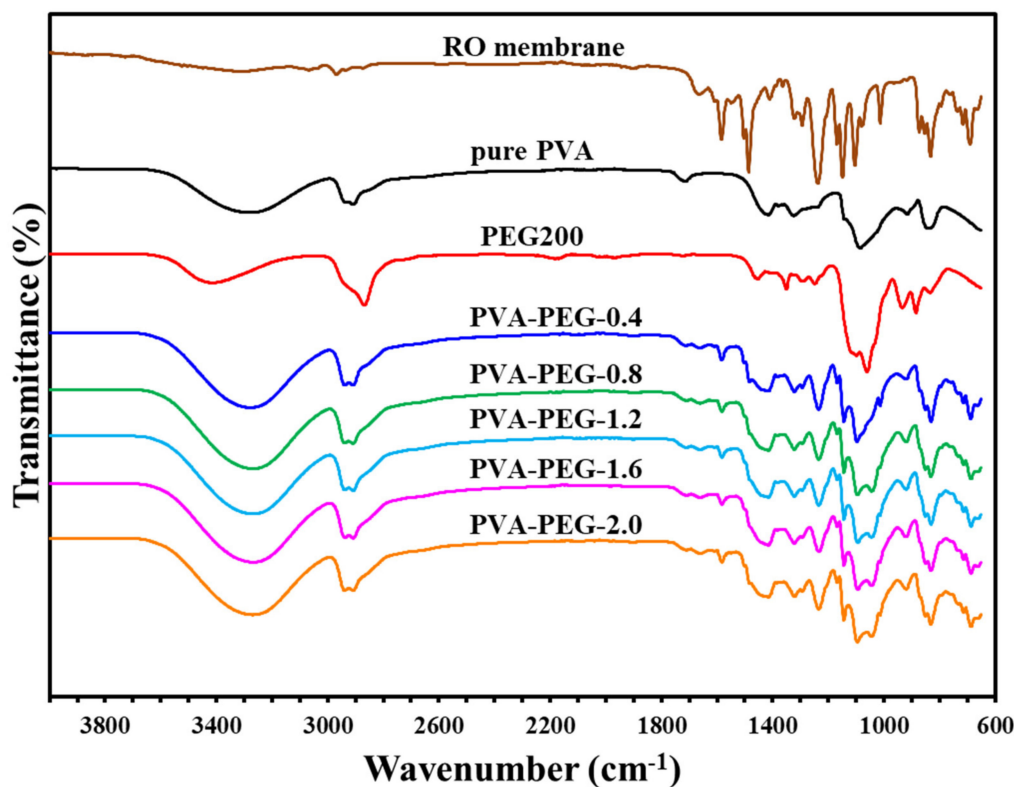


Figure 6. Infrared spectrum of polyvinyl alcohol–polyethylene glycol composite membranes.

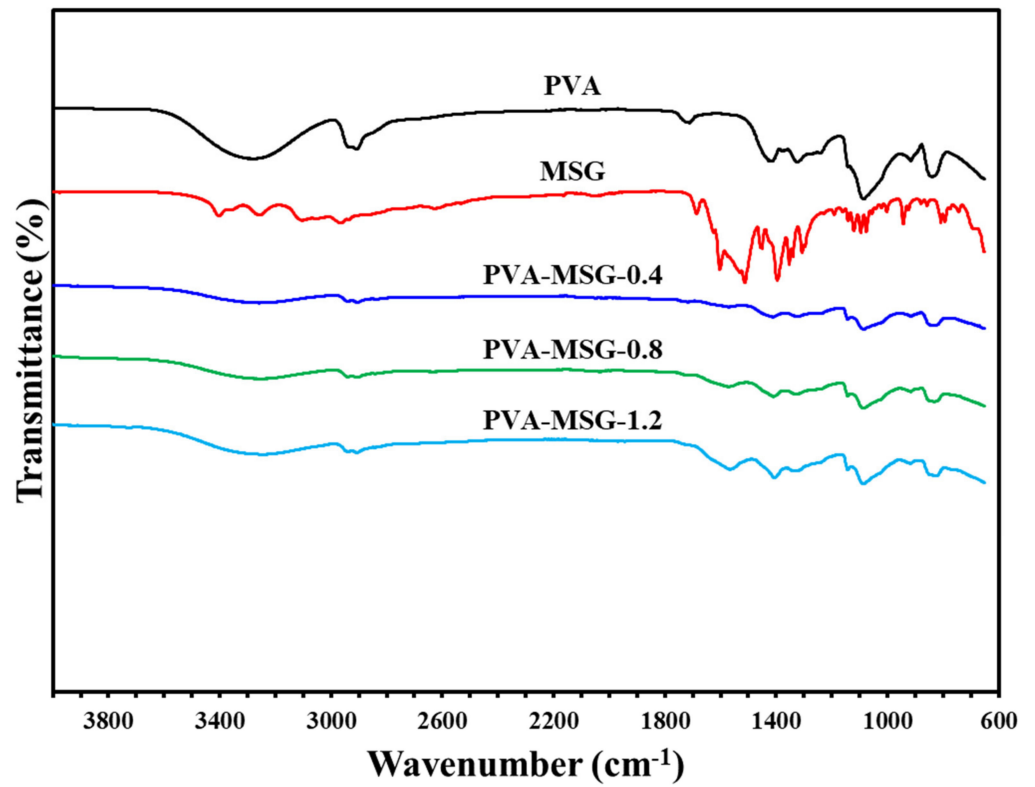


Figure 7. Infrared spectrum of polyvinyl alcohol-sodium glutamate self-supporting membranes.

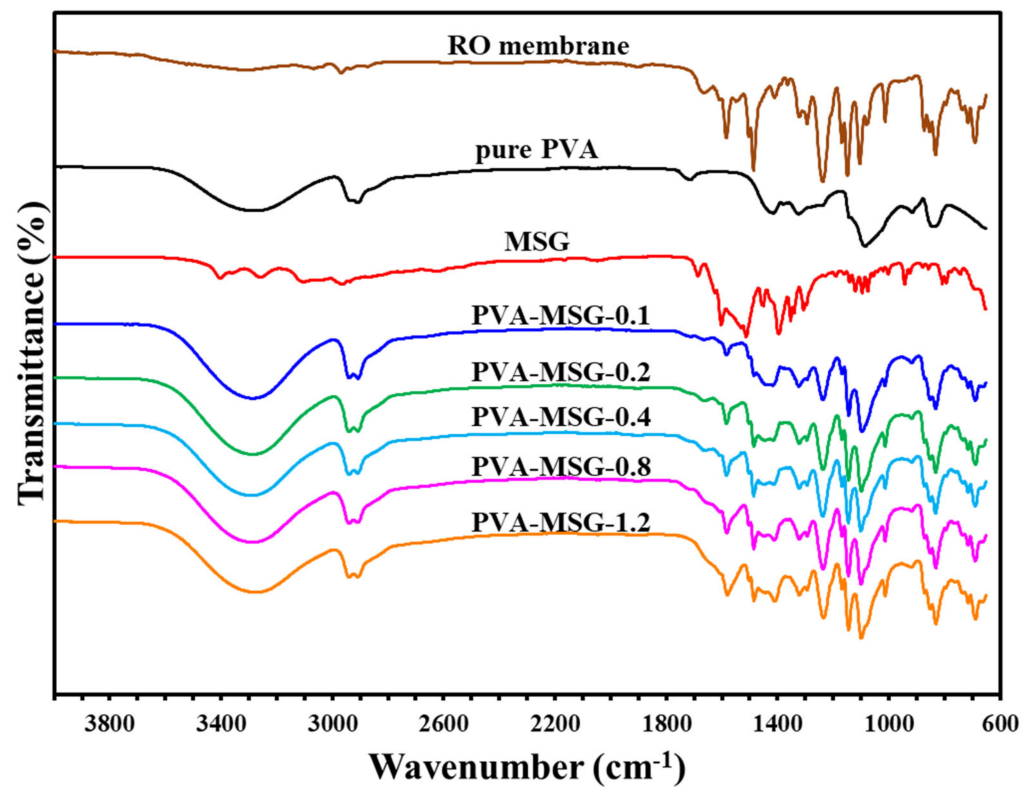


Figure 8. Infrared spectrum of polyvinyl alcohol-sodium glutamate composite membranes.

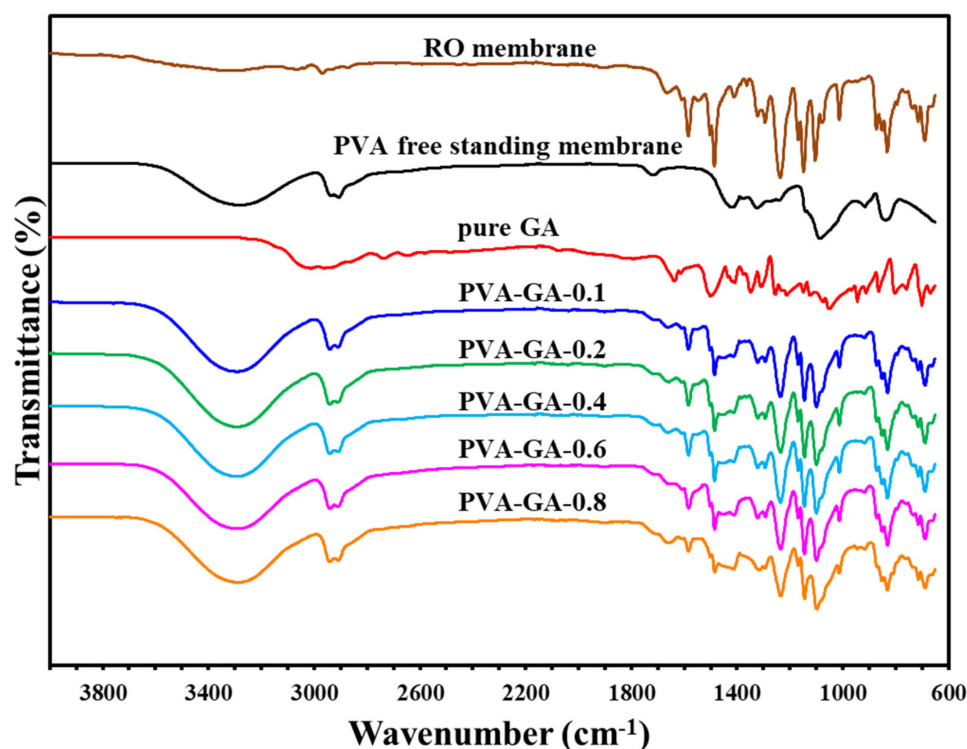


Figure 9. TGA diagram of polyvinyl alcohol–glutamic acid composite membranes.

Table 3. Peak assignments of PVA-X composite membranes.

Peak Position (cm ⁻¹)			Peak Assignment
PVA-PEG	PVA-MSG	PVA-GA	
3000–3600	3000–3600	3000–3600	O-H stretching
2800–2900	2950–3050	2950–3050	C-H stretching
		1635	N-H stretching
	1602		C-O stretching
		1500	N-H stretching, symmetric
		1400	COOH stretching, symmetric
	1395		C-O stretching
1350			C-O stretching
1090			C-O stretching

3.2. Thermogravimetric Analysis

To avoid a weight increase associated with increased thickness of the support material, the polyester support layer in the composite membrane is torn off, leaving only three layers of mixed polymer, polyamide and polyurethane. The thermal stability of the composite membrane is tested under an argon atmosphere with a temperature ramp increasing to 900 °C. Polyvinyl alcohol (PVA)-polyglycol (PEG) composite membrane thermal stability experimental results are shown in Figure 10 and Table 4. It is observed that the reverse osmosis membrane as a substrate has a significant weight loss only at 500–550 °C, which should be associated with the polysulfone that acts as a support layer. The composite membrane coated with PVA-PEG shows three stages of weight change. The first stage weight change at 150–250 °C comes from the loss of composite membrane moisture and PEG cracking, the second stage at 275–350 °C comes from PVA cracking, and the third stage at 500–550 °C is the same as the reverse osmosis membrane which is caused by PSU lysis. The experimental results of the polyvinyl alcohol–glutamic acid (salt) composite membrane thermal analysis are shown in Figure 11. In addition to PSU cracking, a weight change can be seen at 275–375 °C. From Figure 12, the maximum cleavage rate temperatures of

glutamic acid (salt) and PVA are approximately 300–400 °C, so this temperature change should be as a result of the degradation of glutamate acid and PVA.

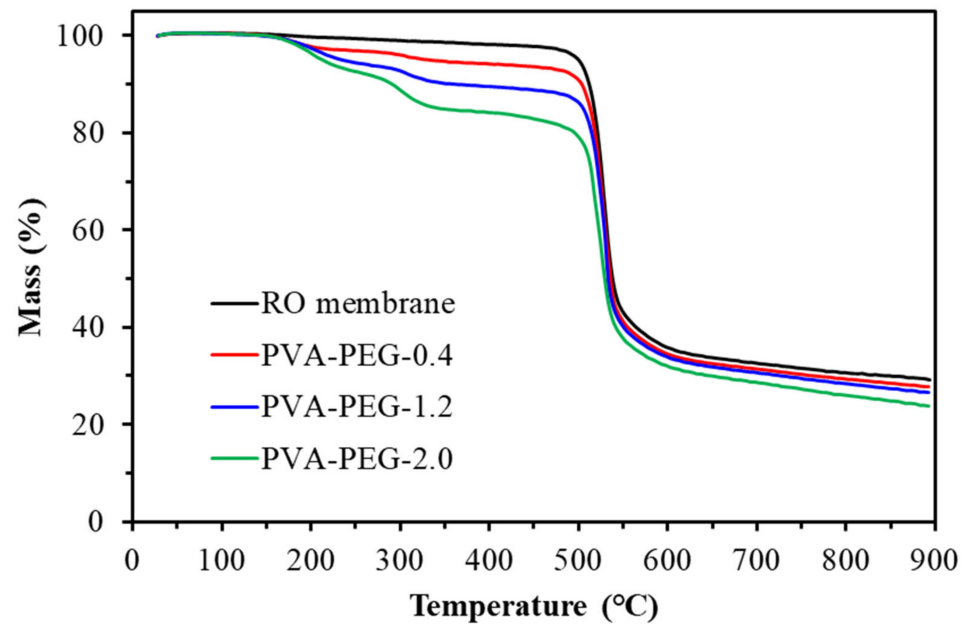


Figure 10. TGA diagram of polyvinyl alcohol-polyethylene glycol composite membranes.

Table 4. Thermal gravimetric analysis.

Sample	1st Degradation		2nd Degradation		3rd Degradation	
	T ₁ (°C)	Weight Loss (%)	T ₂ (°C)	Weight Loss (%)	T ₃ (°C)	Weight Loss (%)
RO	500–550	50	-	-	-	-
PVA-PEG-2.0	150–250	7.3	275–350	5.8	500–550	45.8
PVA-MSG-1.2	275–375	7.7	500–550	51.1	-	-
PVA-GA-0.8	275–375	5.9	500–550	54.0	-	-

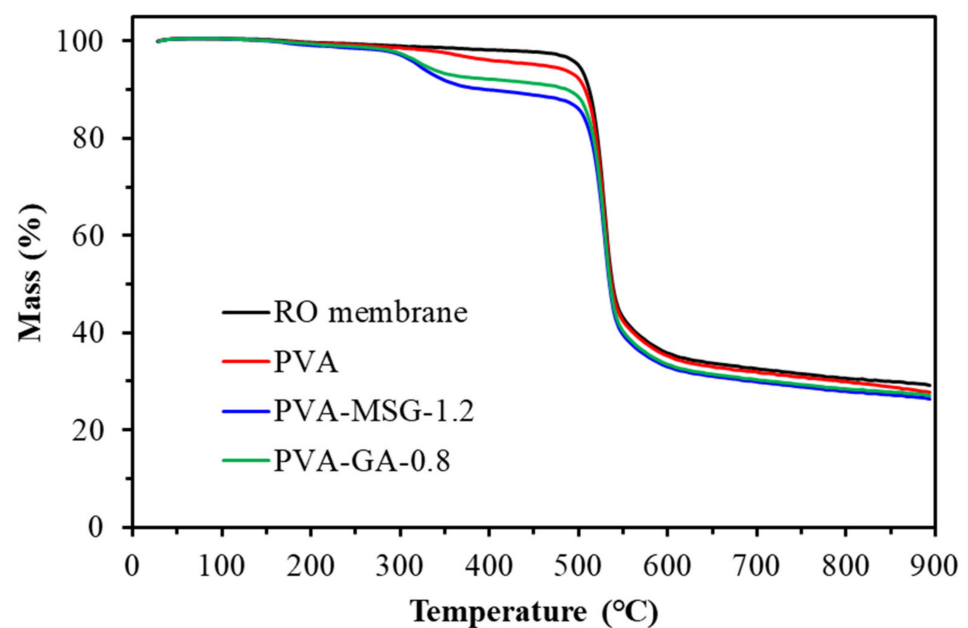


Figure 11. TGA diagram of polyvinyl alcohol-glutamic acid (salt) composite membranes.

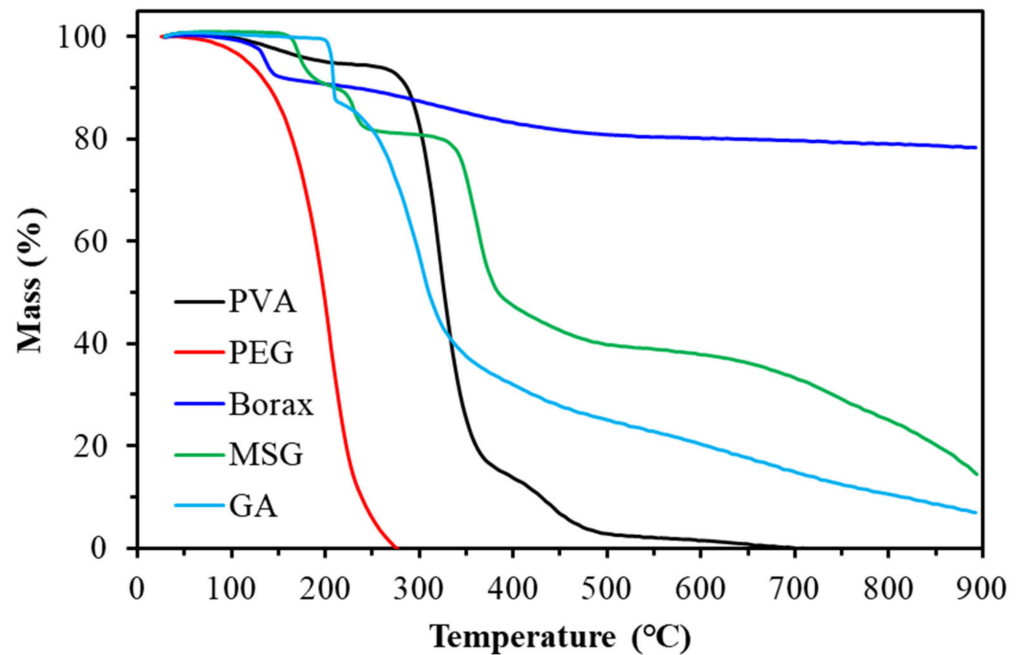


Figure 12. TGA diagram of experimental chemicals.

3.3. SEM Analysis

SEM was used to observe the membrane surface pattern and showed that the polyamide layer distribution as a substrate had many holes, as shown in Figure 13A. When the composite membrane surface is coated with a polyvinyl alcohol solution (PVA-B-2), the original rough surface is covered by PVA and converted to a dense surface as shown in Figure 13B.

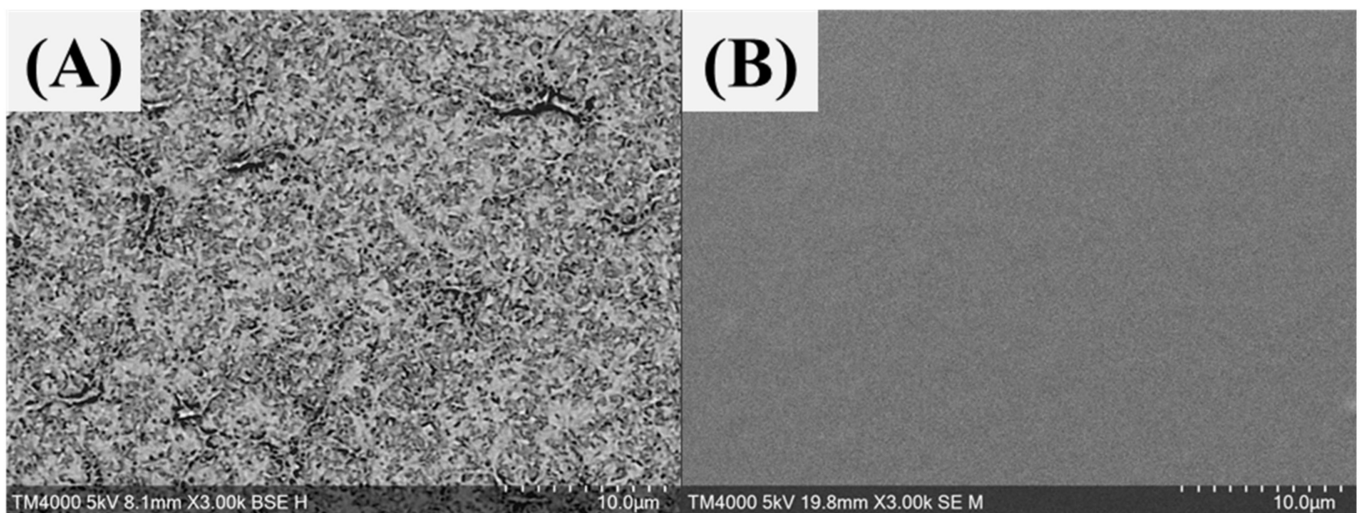


Figure 13. SEM diagrams of (A) reverse osmosis film and (B) PVA-B-2 coated film.

In the PVA-PEG series of polyvinyl alcohols with different proportions of polyglycol, the surface of the coated composite membrane remains dense, no different from the PVA-B-2 condition of the original polyethylene glycol addition as shown in Figure 14.

A PVA-MSG series of samples of polyvinyl alcohol with added sodium glutamate, whose surfaces remain dense when MSG is less than 9 wt% (PVA-MSG-0.4) as shown in Figure 15A–C. From Figure 15D–F, as the MSG addition increases, particles are observed on the membrane surface, and as the amount added increases further, so the particle size becomes larger and more widely distributed. The particles are crystallized MSG distributed on the membrane surface.

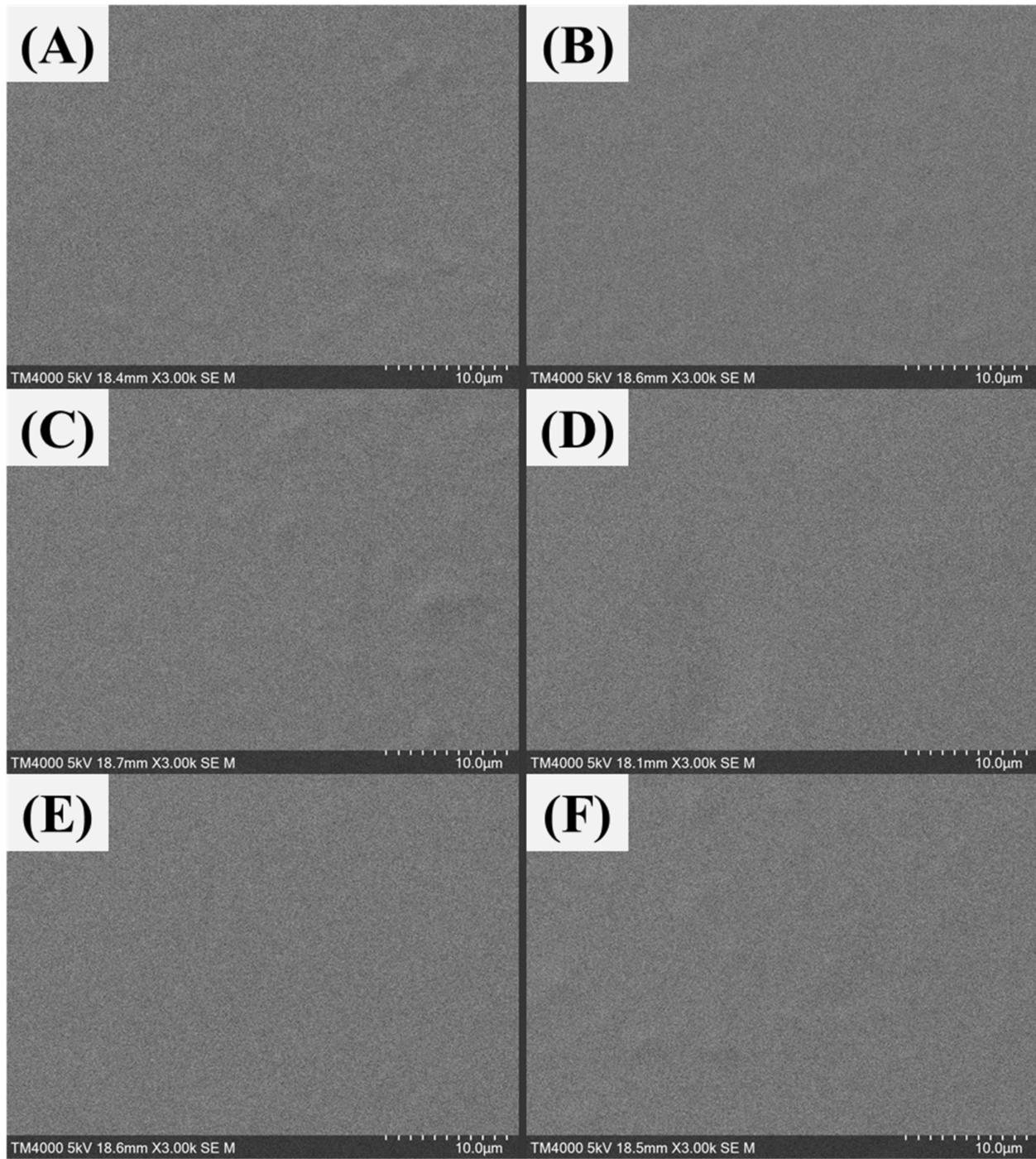


Figure 14. SEM diagrams of different PEG content PVA-PEG composite membranes: (A) no additional PEG, (B) 10 wt%, (C) 18 wt%, (D) 24 wt%, (E) 30 wt%, and (F) 35 wt%.

The coating solution is changed to polyvinyl alcohol to add glutamate acid PVA-GA series samples. The GA addition amount is less than 9 wt% (PVA-GA-0.4). Its surface also appears to be in a dense state as shown in Figure 16A–D. From Figure 16E,F, as the GA addition continues to be increased above 13 wt% (PVA-GA-0.6), granular fluctuations are found on the surface, while at 17 wt%, GA will have larger particles, which result from GA aggregation.

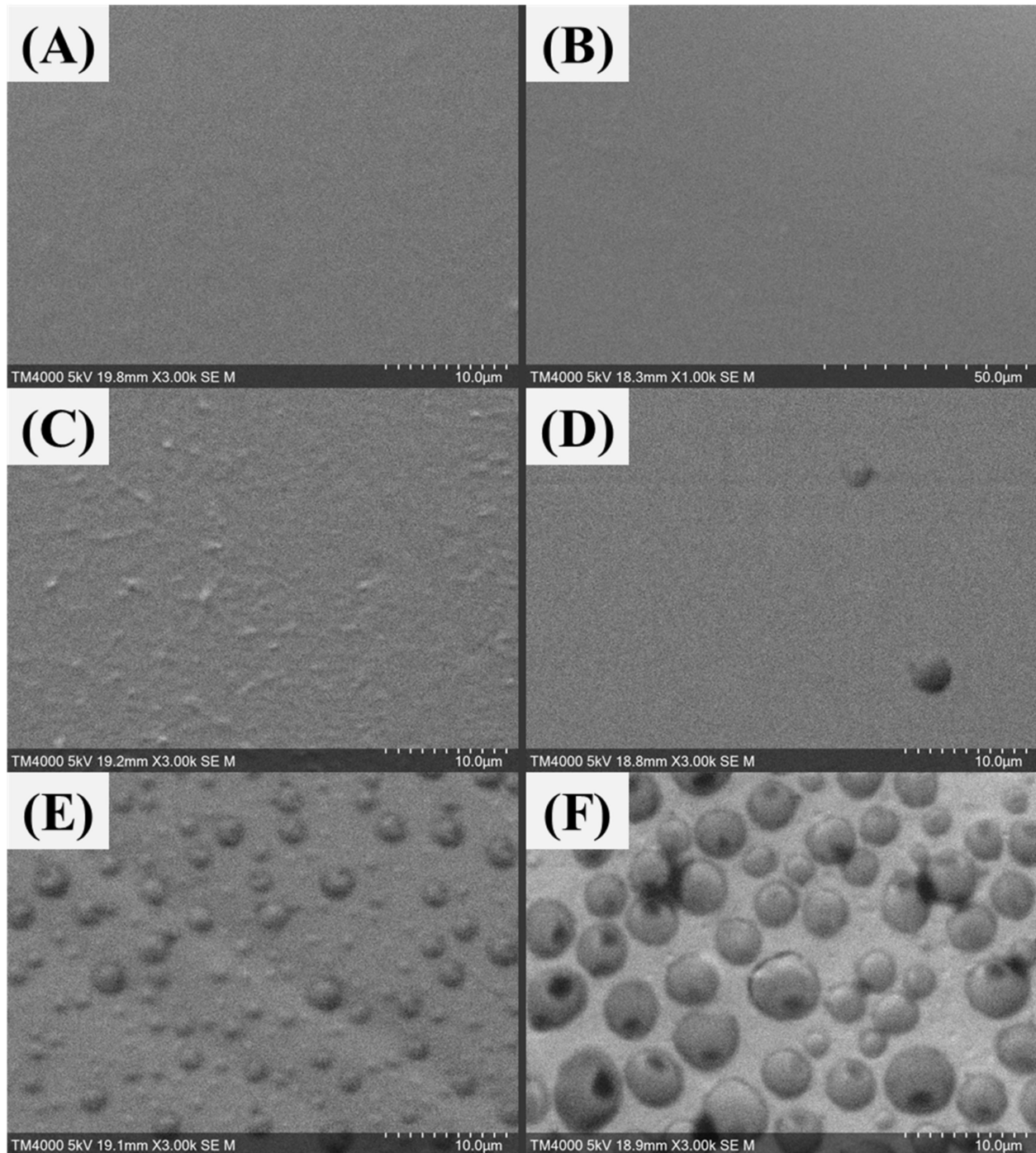


Figure 15. SEM diagrams of different MSG content PVA-MSG composite membranes: (A) no additional MSG, (B) 2 wt%, (C) 5 wt%, (D) 9 wt%, (E) 17 wt%, and (F) 23 wt%.

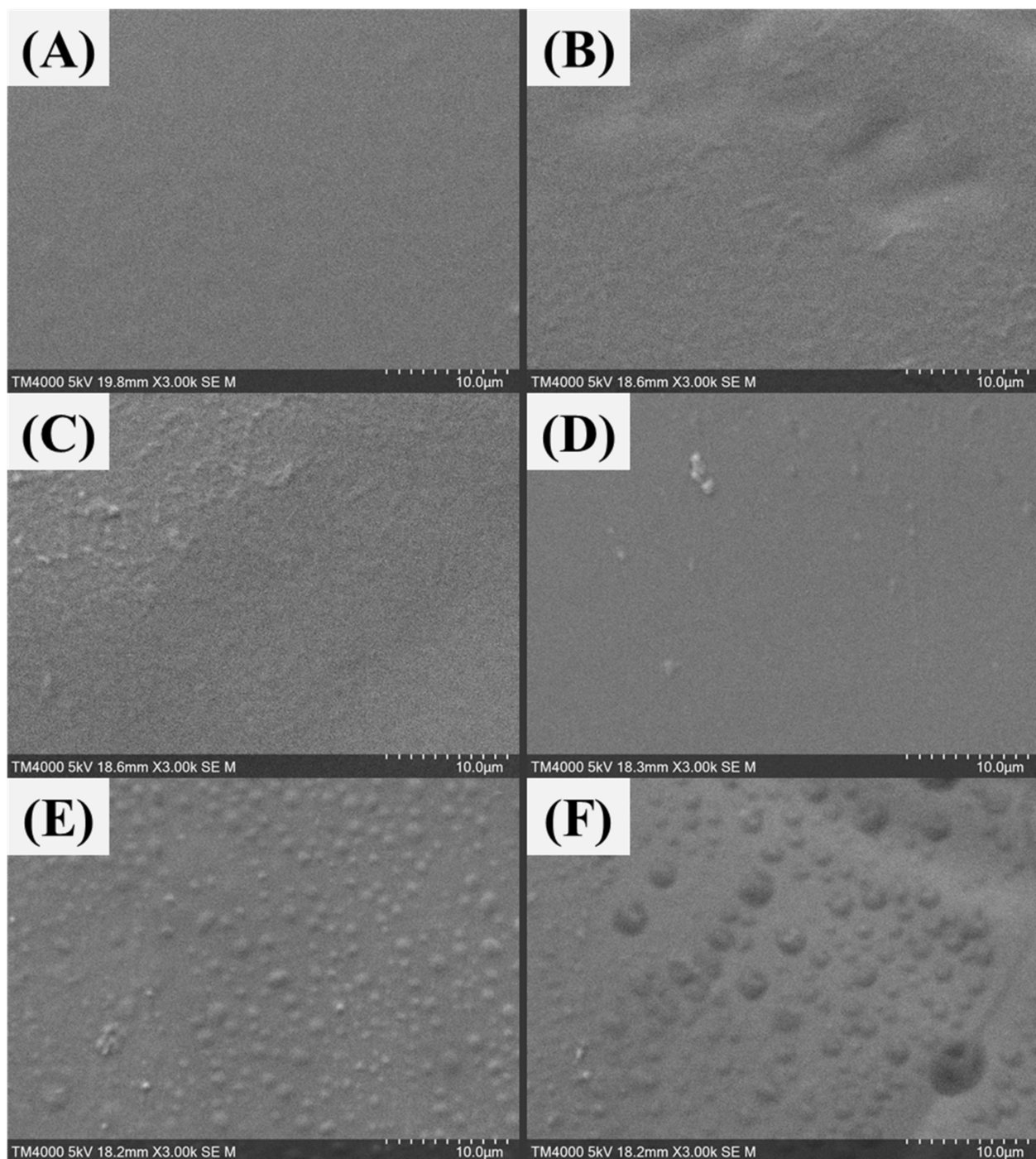


Figure 16. SEM diagrams of different GA content PVA-GA composite membranes: (A) no additional GA, (B) 2 wt%, (C) 5 wt%, (D) 9 wt%, (E) 13 wt%, and (F) 17 wt%.

3.4. Effect of Moisture on the Separation Efficiency of Polyvinyl Alcohol-Polyglycol Composite Membrane

The experimental results are shown in Figure 17 and Tables 5 and 6. In wet environments, CO₂ permeability is improved compared to dry environments, while N₂ permeability decreases slightly compared to dry environments, resulting in a significant improvement in CO₂/N₂ selectivity in wet environments compared with dry environments. This can be attributed to the ambient humidity increasing moisture content in the hydrophilic polyvinyl alcohol membrane, so that CO₂ can react with the water to produce

bicarbonate, accelerating the transmission of CO₂ in the membrane. CO₂ permeability increases, compared with N₂, since water solubility for the latter is small [30,31], making CO₂/N₂ more selective in humid environments than in dry environments.

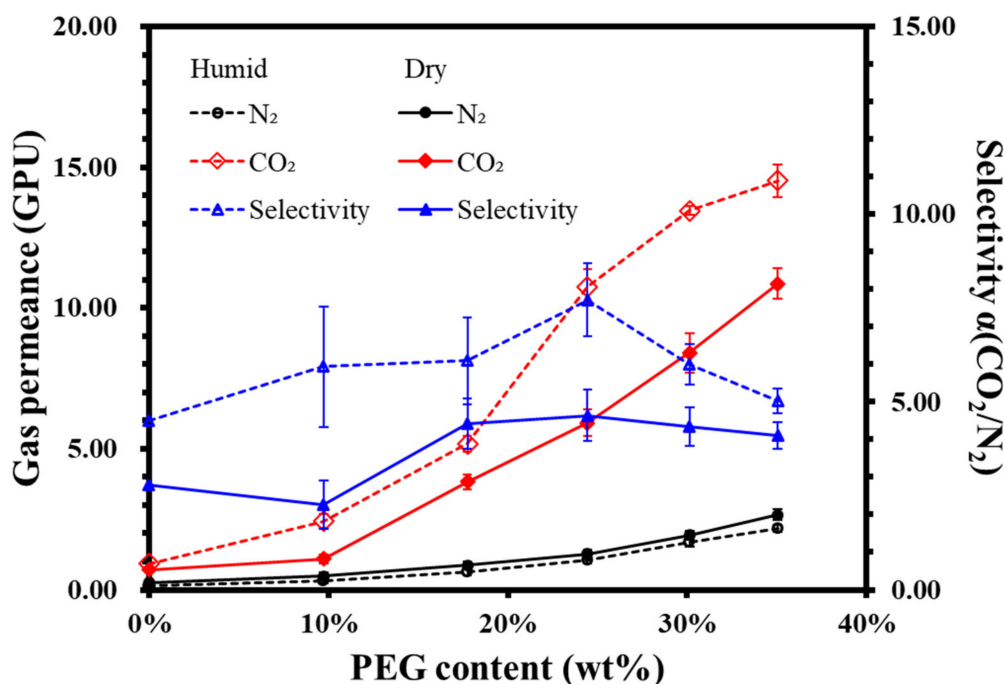


Figure 17. Effect of PEG content on the gas permeability of composite membrane in a dry or humid environment.

Table 5. Gas permeability and selectivity in a dry environment *.

Sample	PEG (wt%)	Permeance (GPU)		Selectivity (CO ₂ /N ₂)
		CO ₂	N ₂	
PVA-B-2	0	0.71 ± 0.12	0.26 ± 0.12	2.80 ± 1.36
PVA-PEG-0.4	10	1.10 ± 0.16	0.48 ± 0.12	2.26 ± 0.63
PVA-PEG-0.8	18	3.83 ± 0.28	0.87 ± 0.12	4.41 ± 0.68
PVA-PEG-1.2	24	5.72 ± 0.25	1.26 ± 0.08	4.53 ± 0.34
PVA-PEG-1.6	30	8.42 ± 0.70	1.94 ± 0.16	4.34 ± 0.51
PVA-PEG-2.0	35	10.86 ± 0.54	2.65 ± 0.19	4.10 ± 0.36

* Feed gas pressure: 1.00 bar.

Table 6. Gas permeability and selectivity in a humid environment *.

Sample	PEG (wt%)	Permeance (GPU)		Selectivity (CO ₂ /N ₂)
		CO ₂	N ₂	
PVA-B-2	0	0.92 ± 0.15	0.15 ± 0.08	6.00 ± 3.16
PVA-PEG-0.4	10	2.42 ± 0.25	0.31 ± 0.08	7.92 ± 2.14
PVA-PEG-0.8	18	5.18 ± 0.27	0.64 ± 0.12	8.12 ± 1.55
PVA-PEG-1.2	24	11.34 ± 0.41	1.13 ± 0.13	10.05 ± 1.22
PVA-PEG-1.6	30	13.46 ± 0.15	1.68 ± 0.15	8.00 ± 0.73
PVA-PEG-2.0	35	14.54 ± 0.58	2.17 ± 0.12	6.71 ± 0.45

* Feed gas pressure: 1.00 bar.

PVA-PEG-1.2 has the best gas selectivity. This composite film was tested under different pressure difference conditions, with results shown in Figure 18 and Table 7. It is observed that the nitrogen permeability of the composite film does not change appreciably, while CO₂ permeability and gas selectivity increase slightly with decreasing pressure difference. This decrease in pressure differential and increase in gas permeability are

usually caused by the promotion of transmission mechanisms [30,32]. This occurs when the gas is passed through the membrane by the dissolve-diffusion mechanism, since its driving force comes from different pressures at both ends of the membrane, resulting in a gas concentration gradient. Calculation of permeability requires division of the pressure difference at both ends, with permeability in the simple solubility-diffusion mechanism assuming no gradient. For a small pressure difference, the proportion of promoting transmission mechanism is larger, and when the pressure difference gradually increases, the carrier molecules with CO₂ gradually reach saturation. At this point, the system is converted from the dissolved-diffusion mechanism to account for a larger proportion. CO₂ permeability will gradually tend to stabilize the constant [32]. There is a negative correlation between CO₂ permeability and the pressure difference.

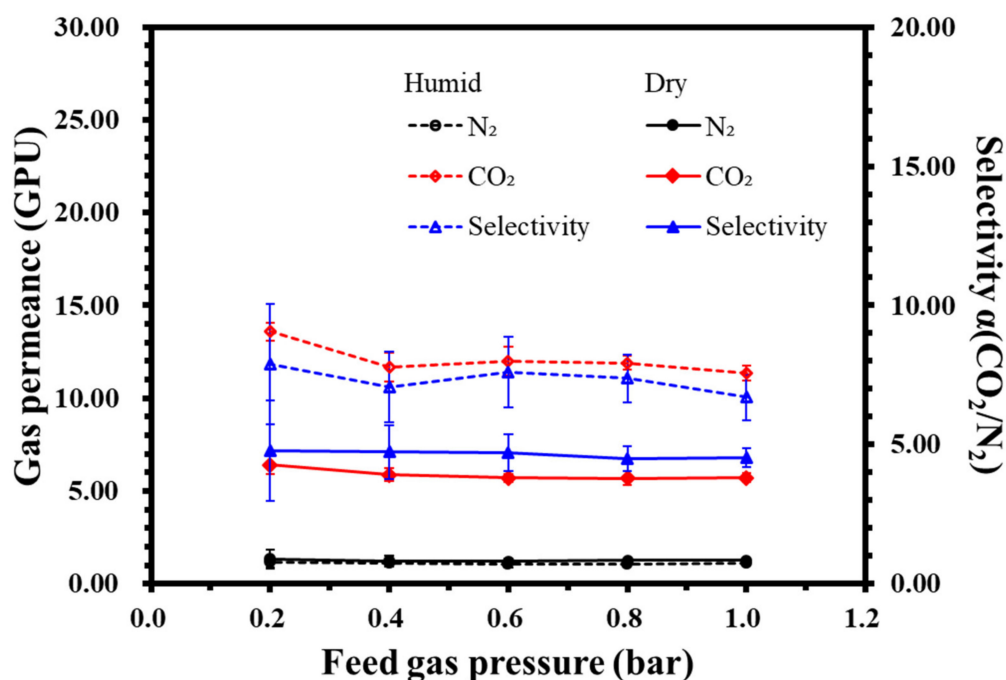


Figure 18. The relationship between gas permeability/selectivity and the pressure of the PVA-PEG-1.2 composite membrane in a dry or humid environment.

Table 7. The gas permeability and selectivity of PVA-PEG-1.2 membrane in varied pressure.

Pressure (bar)	Permeance (GPU)				Selectivity	
	Dry		Humid		Dry	Humid
	CO ₂	N ₂	CO ₂	N ₂	(CO ₂ /N ₂)	(CO ₂ /N ₂)
1.00	5.72 ± 0.25	1.26 ± 0.08	11.34 ± 0.41	1.13 ± 0.13	4.53 ± 0.34	10.05 ± 1.22
0.80	5.69 ± 0.37	1.27 ± 0.09	11.91 ± 0.39	1.08 ± 0.12	4.49 ± 0.44	11.07 ± 1.29
0.60	5.71 ± 0.22	1.21 ± 0.16	11.99 ± 0.79	1.05 ± 0.16	4.71 ± 0.66	11.39 ± 1.89
0.40	5.88 ± 0.33	1.24 ± 0.25	11.67 ± 0.78	1.10 ± 0.18	4.73 ± 0.98	10.61 ± 1.90
0.20	6.41 ± 0.48	1.34 ± 0.49	13.58 ± 0.49	1.15 ± 0.31	4.79 ± 1.80	11.83 ± 3.25

The experimental results show that there should be a transmission mechanism in the polyvinyl alcohol-polyethylene glycol membrane, which may be derived from moisture in the membrane. This is because polyvinyl alcohol is cross-linked, and the relative humidity of the dry environment set by the experiment is still approximately 40%. Whether in a dry environment or humid environment, the membrane still retains moisture to promote the transmission mechanism, so that in the case of reduced CO₂ pressure, CO₂ permeability can increase slightly.

3.5. Effect of Additional Sodium Glutamate and Glutamic Acid on Gas Separation Efficiency

Results from testing additional sodium glutamate in the PVA-MSG membrane are shown in Figure 19 and Table 8. It is observed that with increased MSG content, CO₂ and N₂ permeability also increase. Gas selectivity did not increase appreciably, especially when the MSG content is 23 wt%. N₂ permeability is greatly increased, with gas selectivity falling close to 1. SEM analysis of the composite membrane shows the presence of crystalline MSG on the membrane surface. This results in gaps between PVA and MSG, making it easier for gas to pass through the membrane, thus reducing selectivity [18].

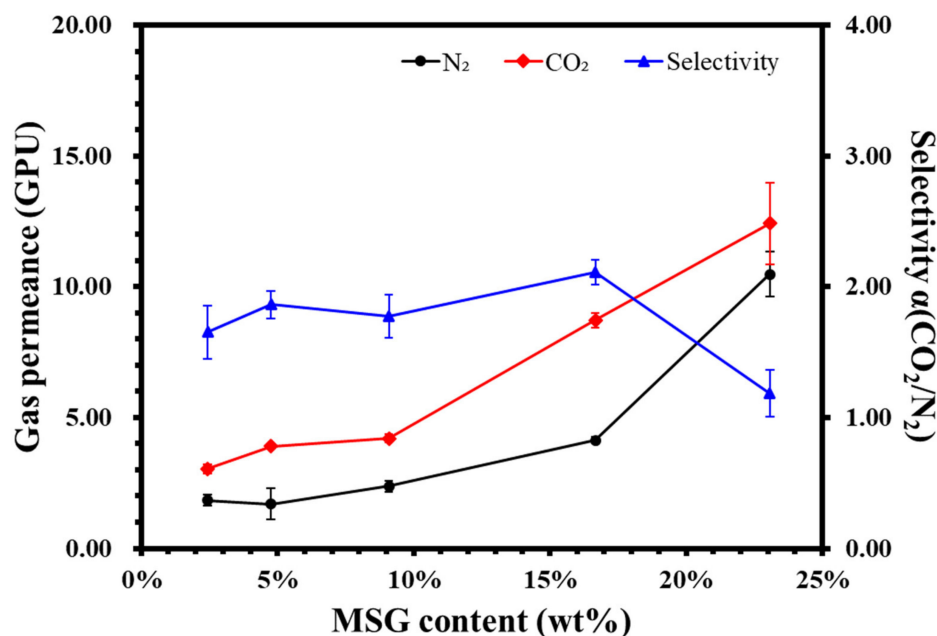


Figure 19. Effect of sodium glutamate content on the gas permeability of composite membrane.

Table 8. Gas permeability of polyvinyl alcohol-sodium glutamate composite membranes *.

Sample	MSG (wt%)	Permeance (GPU)		Selectivity (CO ₂ /N ₂)
		CO ₂	N ₂	
PVA-MSG-0.1	2	3.03 ± 0.16	1.84 ± 0.20	1.65 ± 0.20
PVA-MSG-0.2	5	3.91 ± 0.08	1.69 ± 0.60	1.86 ± 0.10
PVA-MSG-0.4	9	4.21 ± 0.15	2.37 ± 0.20	1.77 ± 0.16
PVA-MSG-0.8	17	8.72 ± 0.27	4.13 ± 0.13	2.11 ± 0.09
PVA-MSG-1.2	23	12.42 ± 1.55	10.48 ± 0.85	1.18 ± 0.18

* Feed gas pressure: 1.00 bar, wet condition.

Results from testing additional glutamate acid in the PVA-GA membrane are shown in Figure 20 and Table 9. Similar to the addition of MSG, CO₂ and N₂ permeability increase with the additional content, but gas selectivity does not increase appreciably. Gas selectivity falls to approximately 1, the reason assumed to be the same as for the PVA-MSG membrane.

Table 9. Gas permeability of polyvinyl alcohol/glutamic acid composite membranes *.

Sample	GA (wt%)	Permeance (GPU)		Selectivity (CO ₂ /N ₂)
		CO ₂	N ₂	
PVA-GA-0.1	2	2.78 ± 0.19	1.76 ± 0.08	1.58 ± 0.13
PVA-GA-0.2	5	2.83 ± 0.15	1.63 ± 0.56	1.46 ± 0.12
PVA-GA-0.4	9	5.43 ± 0.20	2.81 ± 0.12	1.94 ± 0.11
PVA-GA-0.6	13	7.06 ± 0.27	3.85 ± 0.12	1.83 ± 0.09
PVA-GA-0.8	17	7.88 ± 0.20	6.15 ± 0.23	1.28 ± 0.06

* Feed gas pressure: 1.00 bar, wet condition.

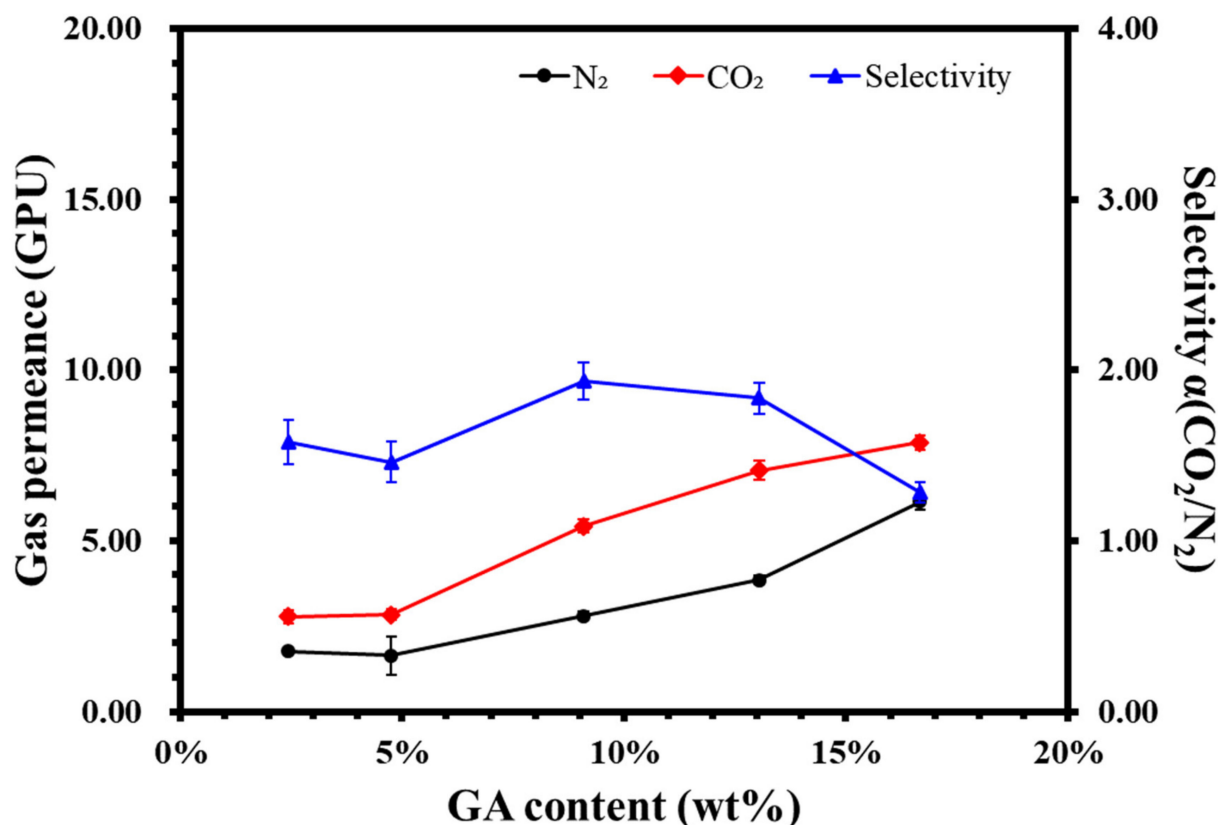


Figure 20. Effect of glutamic acid content on the gas permeability of composite membrane.

3.6. Separation Efficiency of CO₂

Separation efficiency tests for PVA-PEG-1.2, PVA-MSG-0.8, and PVA-GA-0.4 composite membranes were completed. Experimental results are shown in Figure 21 and Table 10. Experiments show that the polyvinyl alcohol-polyethylene glycol as a selection layer coated on the reverse osmosis membrane can improve the concentration of CO₂ passing through this composite membrane. PVA-PEG-1.2 can increase the concentration of CO₂ to approximately 32.6 ppm (composite membrane concentration difference-reverse osmosis membrane concentration difference). The PVA-MSG-0.8 composite membrane and PVA-GA-0.4 composite membranes increased CO₂ concentration by approximately 8.6 ppm and 5.0 ppm, respectively. These results show that the addition of glut amine or glutamate is not a viable option to affect a significant increase in CO₂ concentration.

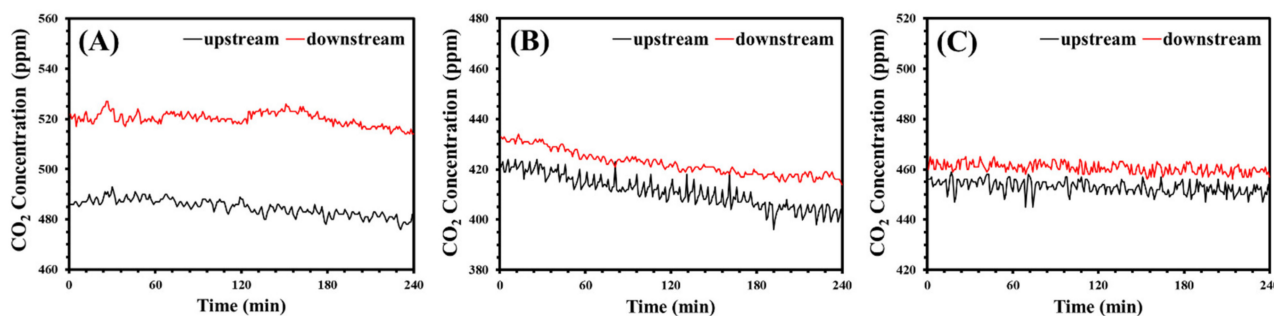


Figure 21. The concentration difference of CO₂ in the composite membranes: (A) PVA-PEG-1.2, (B) PVA-MSG-0.8, and (C) PVA-GA-0.4.

Table 10. Separation efficiency of the composite membranes.

Sample	Pressure Difference (mmHg)	CO ₂ Concentration (ppm)
blank	-	2.43 ± 2.08
reverse osmosis membrane	700	2.73 ± 1.43
PVA-PEG-1.2	700	35.37 ± 3.15
PVA-MSG-0.8	700	11.32 ± 3.32
PVA-GA-0.4	700	7.70 ± 2.76

3.7. Water Absorption of the Membrane

The experimental results of water absorption measurement of the self-supporting membrane are shown in Table 11. The results show that compared with pure polyvinyl alcohol PVA membrane, water absorption of the PVA-B-2 membrane with Borax was increased from 52.3% to 60.7%, while the PVA-PEG-1.2 membrane with polyethylene glycol resulted in a higher increase to 72.1%. In contrast, water absorption of PVA-MSG-0.8 membrane with sodium glutamate decreased.

Table 11. Water absorption measurement of the self-supporting membranes.

Sample	Water Uptake (%)
PVA	52.3 ± 1.4
PVA-B-2	60.7 ± 1.3
PVA-PEG-1.2	72.1 ± 1.6
PVA-MSG-0.8	39.9 ± 1.3
PVA-GA-0.4	N/A

There are two reasons for the decrease in water absorption associated with the addition of sodium glutamate. Firstly, because the water absorptivity of sodium glutamate is less than that of polyvinyl alcohol, the addition of sodium glutamate results in an overall decrease in water absorptivity. Secondly, as observed via SEM analysis, sodium glutamate forms particles on the surface of the membrane, thus reducing the contact area between the membrane and moisture in the space. This results in a decrease in water absorption of the PVA-MSG-0.8 membrane over the same period.

The addition of sodium tetraborate increases water absorption. Sodium tetraborate dissolves in water to form a mixed solution of boric acid and hydrogen and oxygen root ions, increasing the overall pH. In previous studies [30,31] researchers also found that when the PVA membrane is partially alkaline, water absorption of the membrane increased. Polyethylene glycol and polyvinyl alcohol are hydrophilic, while also reducing the crystallization of polyvinyl alcohol [33]. Therefore, water absorption of the PVA-PEG-1.2 membrane is higher than that of the PVA-B-2 membrane.

3.8. The Deterioration Measurement of the Selectivity of CO₂ Membrane

In this experiment, the highest CO₂ selectivity sample of each group, namely PVA-PEG-1.2, PVA-MSG-0.8 and PVA-GA-0.4 composite membrane, were tested. CO₂ selectivity for each material was tested after 48, 96, 144, 192, and 240 h to determine whether the composite membrane has deteriorated over the 10-day period. Experimental results are shown in Figure 22 and Table 12.

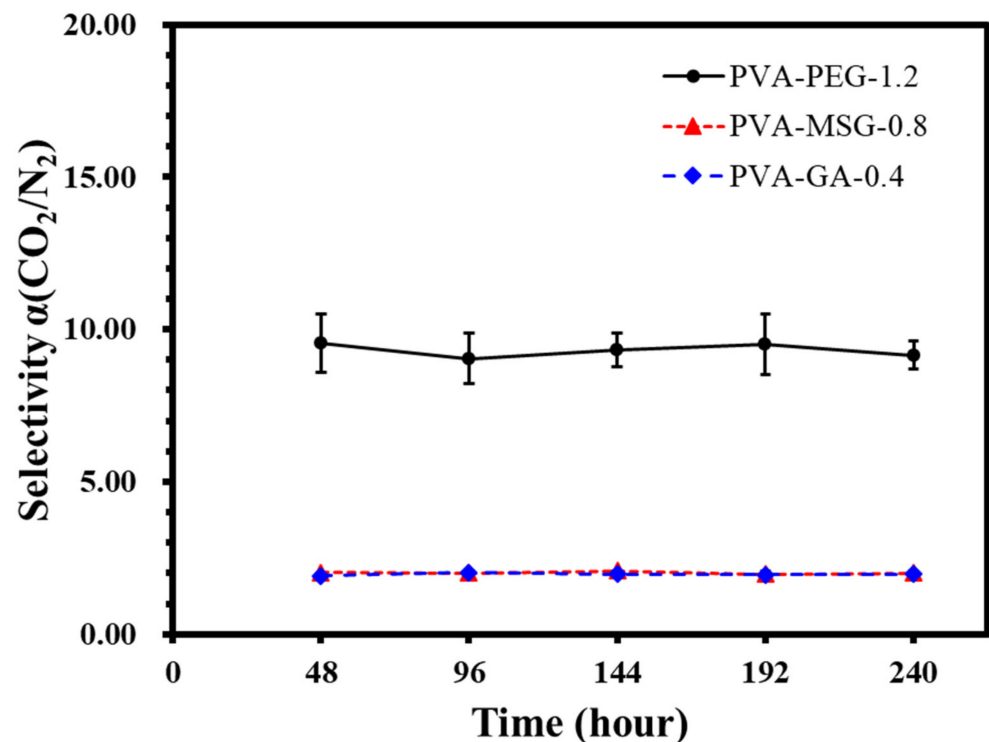


Figure 22. The selectivity of PVA-PEG-1.2, PVA-MSG-0.8, and PVA-GA-0.4 composite membranes.

Table 12. The selectivity $\alpha(\text{CO}_2/\text{N}_2)$ of PVA-X composite membranes.

Time (hour)	PVA-PEG-1.2	PVA-MSG-0.8	PVA-GA-0.4
48	9.59 ± 0.97	2.10 ± 0.08	1.91 ± 0.09
96	9.56 ± 0.95	2.02 ± 0.13	2.01 ± 0.04
144	9.04 ± 0.83	2.01 ± 0.15	1.97 ± 0.11
192	9.33 ± 0.54	1.97 ± 0.09	1.95 ± 0.14
240	9.51 ± 0.99	2.01 ± 0.10	1.97 ± 0.09

Polyvinyl alcohol-polyethylene glycol is measured using PVA-PEG-1.2 composite membrane. The results showed that the selectivity of the gas composite membrane is approximately 9.5. There was no upward or downward trend, and no significant change occurred in 10 days.

Polyvinyl alcohol-sodium glutamate is measured using PVA-MSG-0.8 composite membrane. The results showed that the selectivity of the gas composite membrane is approximately 2.0. There was no upward or downward trend, and no significant change occurred in 10 days.

Polyvinyl alcohol-glutamic acid is measured using PVA-GA-0.4 composite membrane. The results showed that the selectivity of the gas composite membrane is approximately 1.9–2.0. There was no upward or downward trend, and no significant change occurred in 10 days.

3.9. Add Sodium Tetraborate (Borax) Crosslinking Effect

The best gas selectivity PVA-PEG-1.2 was selected as the control group. The material was also formulated using the same polyvinyl alcohol, polyethylene glycol ratio. The sample without Borax, PVA-PEG-1.2-NB, was prepared but with 15 mL Borax solution replaced by deionized water. Its formulation ratio is shown in Table 13. Gas permeability, gas selectivity and moisture adsorption measurement results are shown in Table 14. The experimental results showed that PVA-PEG-1.2 samples with Borax were higher in

PVA-PEG-1.2-NB without Borax, but the gas selectivity was lower and moisture absorption was reduced.

Table 13. The composition of samples with or without Borax.

Sample	PVA (g)	PEG (mL)	Borax (g)
PVA-PEG-1.2	4.00	1.20	0.08
PVA-PEG-1.2-NB	4.00	1.20	-

Table 14. The gas separation and adsorption properties of samples with or without Borax.

Sample	Permeance (GPU)		Selectivity (CO ₂ /N ₂)	Water Uptake (%)
	CO ₂	N ₂		
PVA-PEG-1.2	10.76 ± 0.61	1.05 ± 0.12	10.05 ± 1.22	72.1 ± 1.6
PVA-PEG-1.2-NB	13.95 ± 0.42	1.66 ± 0.12	8.42 ± 0.65	66.9 ± 1.7

The PVA-PEG-1.2 composite membrane with Borax added may have better CO₂/N₂ separation than PVA-PEG-1.2-NB without Borax: (1) It can be seen that the power radius of CO₂ is 3.30, and the power radius of nitrogen is 3.64, so crosslinking may cause the membrane aperture and quantity to decrease. The result is that the gas dynamic radius of N₂ is more affected, and permeability decreases more than for CO₂, resulting in a selective increase in CO₂/N₂, as shown in Table 15. (2) It can be seen from the water adsorption experiment that PVA-PEG-1.2 is slightly higher than that of PVA-PEG-1.2-NB, which means it is easier to dissolve into the membrane because of the high solubility of CO₂ in water, resulting in a selectivity increase in CO₂/N₂.

Table 15. Gas dynamic radius.

Molecule	Kinetic Diameter (Å)
CO ₂	3.30
N ₂	3.64

Simulation results of a linear addition of thermal weight changes in each component are shown in Figure 23. It can be seen that PVA-PEG produced significant weight changes in three stages. These occurred at approximately 125 °C, 200–350 °C and 375–450 °C, corresponding to moisture loss, lysis of polyglycol and polyvinyl alcohol branch chains, and cracking of polyvinyl alcohol main chains, respectively [25,34–36].

Comparing the simulated thermal weight loss with the actual experimental results, it is found that with polyethylene glycol mixed into polyvinyl alcohol, the original lysis of polyethylene glycol occurs at a reduced temperature of approximately 200 °C. Secondly, comparing PVA-PEG-1.2 with sodium tetraborate and PVA-PEG-1.2-NB without sodium tetraborate, it can be found that the residual weight of PVA-PEG-1.2 is slightly higher than PVA-PEG-1.2-NB. In addition, the residual weight of PVA-PEG-1.2 is higher before and after 400 °C, which is approximately 10% higher than the simulated thermal weight loss. The B-O-C bond is produced by the crosslinking of boric acid and hydroxyl, so that the polyvinyl alcohol branch chain is less, which could be cracked in this temperature range, resulting in a higher residual weight. Therefore, the use of Borax as a polyvinyl alcohol crosslinking agent can improve the thermal stability of the membrane.

From the experimental results, it can be seen that the use of Borax as a polyvinyl alcohol crosslinking agent, results in a slight decrease in carbon dioxide permeability, and an improvement in CO₂/N₂ selectivity, moisture adsorption and thermal stability. Polyvinyl alcohol is an improvement over other crosslinkers since, unlike formaldehyde, dialdehyde and other commonly used compounds, it can function at room temperature. Therefore, Borax and polyvinyl alcohol can be recommended for the purpose of manufacturing composite membranes suitable for CO₂ separation.

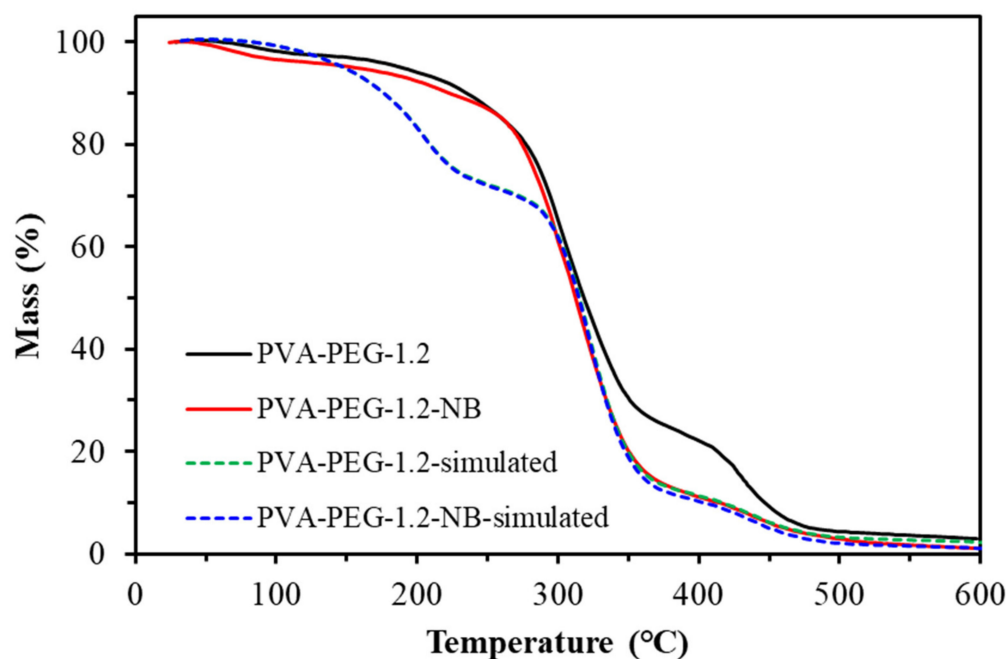


Figure 23. Thermal mass of the PVA-PEG-1.2 composite membrane.

4. Conclusions

In this study, the use of polyethylene glycol, glutamic acid, monosodium glutamate, water as a solvent and polyvinyl alcohol formulated a polymer mixing solution, coated to the surface of the dry reverse osmosis membrane, thereby improving carbon dioxide permeability and CO_2/N_2 selectivity. The addition of polyethylene glycol and glutamic acid (salt) to polyvinyl alcohol films can increase CO_2 permeability. In a humid environment, because moisture promotes the composite membrane transmission mechanism, CO_2 permeability and gas selectivity are higher than in a dry environment. PVA-PEG-1.2 composite membrane is the best selection for CO_2 separation under the condition of a pressure difference of 1.00 bar and a humid environment, the selectivity reaching to 10.05. As PEG content continues to increase, nitrogen permeability increases by more than CO_2 permeability, which leads to a decrease in selectivity. Glutamic acid (salt) may crystallize due to low solubility. The solubility of the amine-based acid itself should be considered when using amine-based acids in polyvinyl alcohol membrane preparation. During the 10-day test, the CO_2/N_2 selectivity of polyvinyl alcohol complex membranes, whether added to polyethylene glycol, sodium glutamate or glutamic acid, remained stable without degradation. Borax can be cross-linked at room temperature and can improve CO_2/N_2 selectivity, water absorption and thermal stability, which can be used by polyvinyl alcohol as the main CO_2 separation membrane.

Author Contributions: Conceptualization, S.-M.C.; data curation, M.-H.T.; formal analysis and investigation, A.S. and M.-H.T.; project administration, S.-M.C. and M.-J.Y.; supervision, S.-M.C. and M.-J.Y.; writing—original draft, M.-H.T. and A.S.; writing—review and editing, S.-M.C. and G.L. All authors have read and agreed to the published version of the manuscript.

Funding: This research was funded by the Ministry of Science and Technology of Taiwan (MOST-107-2221-E-027-027) and the National Taipei University of Technology - Beijing University of Technology Joint Research Program (NTUT-BJUT-110-03; BJUT-NTUT-110-03).

Institutional Review Board Statement: Not applicable.

Informed Consent Statement: Not applicable.

Conflicts of Interest: The authors declare no conflict of interest.

References

1. Lu, J.G.; Cheng, M.; Ji, Y.; Hui, Z. Membrane-based CO₂ absorption into blended amine solutions. *J. Fuel Chem. Technol.* **2009**, *37*, 740–746. [[CrossRef](#)]
2. Bernardo, P.; Drioli, E.; Golemme, G. Membrane Gas Separation: A Review/State of the Art. *Ind. Eng. Chem. Res.* **2009**, *48*, 4638–4663. [[CrossRef](#)]
3. Metz, B.; Davidson, O.; De Coninck, H.C.; Loos, M.; Meyer, L. *IPCC Special Report on Carbon Dioxide Capture and Storage, Intergovernmental Panel on Climate Change (IPCC)*; Cambridge University Press: Cambridge, UK, 2005; p. 442.
4. Suleman, M.S.; Lau, K.K.; Yeong, Y.F. Plasticization and Swelling in Polymeric Membranes in CO₂ Removal from Natural Gas. *Chem. Eng. Technol.* **2016**, *39*, 1604–1616. [[CrossRef](#)]
5. Lin, H.; Freeman, B.D. Materials selection guidelines for membranes that remove CO₂ from gas mixtures. *J. Mol. Struct.* **2005**, *739*, 57–74. [[CrossRef](#)]
6. Klaassen, R.; Feron, P.H.M.; Jansen, A.E. Membrane Contactors in Industrial Applications. *Chem. Eng. Res. Des.* **2005**, *83*, 234–246. [[CrossRef](#)]
7. He, X.; Yu, Q.; Hägg, M.B. CO₂ Capture. In *Encyclopedia of Membrane Science and Technology*; Hoek, E.M.V., Tarabara, V.V., Eds.; Wiley: Hoboken, NJ, USA, 2013.
8. Freeman, B.D. Basis of permeability/selectivity tradeoff relations in polymeric gas separation membranes. *Macromolecules* **1999**, *32*, 375–380. [[CrossRef](#)]
9. Robeson, L.M. The upper bound revisited. *J. Membr. Sci.* **2008**, *320*, 390–400. [[CrossRef](#)]
10. Baker, R.W.; Low, B.T. Gas separation membrane materials: A perspective. *Macromolecules* **2014**, *47*, 6999–7013. [[CrossRef](#)]
11. Chung, T.S. A review of microporous composite polymeric membrane technology for air-separation. *Polym. Polym. Compos* **1996**, *4*, 269–283.
12. Dai, Z.; Ansaloni, L.; Deng, L. Recent advances in multi-layer composite polymeric membranes for CO₂ separation: A review. *Green Energy Environ.* **2016**, *1*, 102–128. [[CrossRef](#)]
13. Li, P.; Chen, H.Z.; Chung, T.S. The effects of substrate characteristics and pre-wetting agents on PAN-PDMS composite hollow fiber membranes for CO₂/N₂ and O₂/N₂ separation. *J. Membr. Sci.* **2013**, *434*, 18–25. [[CrossRef](#)]
14. Xie, K.; Fu, Q.; Qiao, G.G.; Webley, P.A. Recent progress on fabrication methods of polymeric thin film gas separation membranes for CO₂ capture. *J. Membr. Sci.* **2019**, *572*, 38–60. [[CrossRef](#)]
15. Sun, J.; Yi, Z.; Zhao, X.; Zhou, Y.; Gao, C. CO₂ separation membranes with high permeability and CO₂/N₂ selectivity prepared by electrostatic self-assembly of polyethylenimine on reverse osmosis membranes. *RSC Adv.* **2017**, *7*, 14678–14687. [[CrossRef](#)]
16. Zou, J.; Ho, W.S.W. CO₂-selective polymeric membranes containing amines in crosslinked poly(vinyl alcohol). *J. Membr. Sci.* **2006**, *286*, 310–321. [[CrossRef](#)]
17. Zhao, Y.; Ho, W.S.W. CO₂-Selective Membranes Containing Sterically Hindered Amines for CO₂/H₂ Separation. *Ind. Eng. Chem. Res.* **2013**, *52*, 8774–8782. [[CrossRef](#)]
18. Zhao, Y.; Ho, W.S.W. Steric hindrance effect on amine demonstrated in solid polymer membranes for CO₂ transport. *J. Membr. Sci.* **2012**, *415–416*, 132–138. [[CrossRef](#)]
19. Xing, R.; Ho, W.S.W. Crosslinked polyvinylalcohol-polysiloxane/fumed silica mixed matrix membranes containing amines for CO₂/H₂ separation. *J. Membr. Sci.* **2011**, *367*, 91–102. [[CrossRef](#)]
20. Zhao, Y.; Jung, B.T.; Ansaloni, L.; Ho, W.S.W. Multiwalled carbon nanotube mixed matrix membranes containing amines for high pressure CO₂/H₂ separation. *J. Membr. Sci.* **2014**, *459*, 233–243. [[CrossRef](#)]
21. Mondal, A.; Mandal, B. Synthesis and characterization of crosslinked poly(vinyl alcohol)/poly(allylamine)/2-amino-2-hydroxymethyl-1,3-propanediol/polysulfone composite membrane for CO₂/N₂ separation. *J. Membr. Sci.* **2013**, *446*, 383–394. [[CrossRef](#)]
22. Cai, Y.; Wang, Z.; Yi, C.; Bai, Y.; Wang, J.; Wang, S. Gas transport property of polyallylamine–poly(vinyl alcohol)/polysulfone composite membranes. *J. Membr. Sci.* **2008**, *310*, 184–196. [[CrossRef](#)]
23. Brunetti, A.; Scura, F.; Barbieri, G.; Drioli, E. Membrane technologies for CO₂ separation. *J. Membr. Sci.* **2010**, *359*, 115–125. [[CrossRef](#)]
24. Hirayama, Y.; Kase, Y.; Tanihara, R.; Sumiyama, Y.; Kusuki, Y.; Haraya, K. Permeation properties to CO₂ and N₂ of poly(ethylene oxide)-containing and crosslinked polymer films. *J. Membr. Sci.* **1999**, *160*, 87–99. [[CrossRef](#)]
25. Potreck, J.; Nijmeijer, K.; Kosinski, T.; Wessling, M. Mixed water vapor/gas transport through the rubbery polymer PEBAX (R) 1074. *J. Membr. Sci.* **2009**, *338*, 11–16. [[CrossRef](#)]
26. Chen, C.; Chen, Y.; Xie, J.; Xu, Z.; Tang, Z.; Yang, F.; Fu, K. Effects of montmorillonite on the properties of cross-linked poly(vinyl alcohol)/boric acid films. *Prog. Org. Coat.* **2017**, *112*, 66–74. [[CrossRef](#)]
27. Lim, M.; Kwon, H.; Kim, D.; Seo, J.; Han, H.; Khan, S.B. Highly-enhanced water resistant and oxygen barrier properties of cross-linked poly(vinyl alcohol) hybrid films for packaging applications. *Prog. Org. Coat.* **2015**, *85*, 68–75. [[CrossRef](#)]
28. Rashidzadeh, M.; Fathi, A.; Ehsani, N.; Baharvandi, H.; Rahimnejad Yazdi, A. Synthesis of Boron Carbide Nano Particles Using Polyvinyl Alcohol and Boric Acid. *Ceram-Silikaty* **2012**, *56*, 32–35.
29. Singh, K.; Devi, S.; Bajaj, H.C.; Ingole, P.; Choudhari, J.; Bhrambhatt, H. Optical Resolution of Racemic Mixtures of Amino Acids through Nanofiltration Membrane Process. *Sep. Sci. Technol.* **2014**, *49*, 2630–2641. [[CrossRef](#)]

30. Roddick-Lanzilotta, A.D.; McQuillan, A.J. An in situ Infrared Spectroscopic Study of Glutamic Acid and of Aspartic Acid Adsorbed on TiO₂: Implications for the Biocompatibility of Titanium. *J. Colloid Interface Sci.* **2000**, *227*, 48–54. [[CrossRef](#)]
31. Saeed, M.; Rafiq, S.; Bergersen, L.H.; Deng, L. Tailoring of water swollen PVA membrane for hosting carriers in CO₂ facilitated transport membranes. *Sep. Purif. Technol.* **2017**, *179*, 550–560. [[CrossRef](#)]
32. Saeed, M.; Deng, L. Carbon nanotube enhanced PVA-mimic enzyme membrane for post-combustion CO₂ capture. *Int. J. Greenh. Gas. Control.* **2016**, *53*, 254–262. [[CrossRef](#)]
33. Deng, L.; Kim, T.J.; Hägg, M.B. Facilitated transport of CO₂ in novel PVAm/PVA blend membrane. *J. Membr. Sci.* **2009**, *340*, 154–163. [[CrossRef](#)]
34. Entezam, M.; Daneshian, H.; Nasirizadeh, N.; Khonakdar, H.A.; Jafari, S.H. Hybrid Hydrogels Based on Poly(vinyl alcohol) (PVA)/Agar/Poly (ethylene glycol) (PEG) Prepared by High Energy Electron Beam Irradiation: Investigation of Physico-Mechanical and Rheological Properties. *Macromol. Mater. Eng.* **2017**, *302*, 1600397. [[CrossRef](#)]
35. Barooah, M.; Mandal, B. Enhanced CO₂ separation performance by PVA/PEG/silica mixed matrix membrane. *J. Appl. Polym. Sci.* **2018**, *135*, 46481. [[CrossRef](#)]
36. Dilshad, M.R.; Islam, A.; Sabir, A.; Shafiq, M.; Butt, M.T.Z.; Ijaz, A.; Jamil, T. Fabrication and performance characterization of novel zinc oxide filled cross-linked PVA/PEG 600 blended membranes for CO₂/N₂ separation. *J. Ind. Eng. Chem.* **2017**, *55*, 65–73. [[CrossRef](#)]